Inorganic Chemistry

Article

pubs.acs.org/IC

Reactivity of the Anionic Diphosphorus Complex $[Mo_2Cp_2(\mu\text{-}PCy_2)(CO)_2(\mu\text{-}\kappa^2\text{:}\kappa^2\text{-}P_2)]^-$ Toward ER_3X Electrophiles (E = C to Pb): Insights into the Multisite Donor Ability and Dynamics of the P_2 Ligand

M. Angeles Alvarez,[†] M. Esther García,[†] Daniel García-Vivó,[†] Alberto Ramos,*[,†] and Miguel A. Ruiz*[,†]

[†]Departamento de Química Orgánica e Inorgánica/IUQOEM, Universidad de Oviedo, E-33071 Oviedo, Spain

Supporting Information

ABSTRACT: The Li^+ salt of the unsaturated anion $[Mo_2Cp_2(\mu\text{-}PCy_2)(\mu\text{-}CO)_2]^-$ reacted with P_4 in tetrahydrofuran at room temperature to give the title complex. This fluxional anion reacted with MeI and $ClCH_2Ph$ to give the diphosphenyl complexes $[Mo_2Cp_2(\mu\text{-}\kappa^2\text{:}\kappa^2\text{-}P_2CH_2R)(\mu\text{-}PCy_2)(CO)_2]$ (R = H, Ph), with the incoming electrophile being attached at the basal P atom of the Mo_2P_2 tetrahedron via the lone electron pair (P−P−CH_3 = 122.8(1)°). In contrast, reactions with $ClER_3$ (ER_3 = $GePh_3$, $SnPh_3$, $PbMe_3$, $PbPh_3$) gave neutral complexes $[Mo_2Cp_2(\mu\text{-}\kappa^2\text{:}\kappa^2\text{-}P_2ER_3)(\mu\text{-}PCy_2)(CO)_2]$ having the incoming electrophile attached at the basal P atom but defining an acute P−P−E angle close to 90° with elongated P−P lengths of ca. 2.20 Å. These complexes undergo an easy fluxional process involving an exchange of the ER_3 group between the P atoms that could be properly modeled through DFT calculations, and some of them displayed minor isomers in solution. Their structure could be rationalized as derived from the interaction of the electrophile with high-energy orbitals of the anion having both σ(Mo−P) and π(P−P) bonding character. Reaction with $BrSiMe_3$ gave instead the agostic phosphenyl complex $[Mo_2Cp_2(\mu\text{-}\kappa^2\text{:}\kappa^1,\eta^2\text{-}HP_2)(\mu\text{-}PCy_2)(CO)_2]$, formally derived from the attachment of a proton to a basal Mo−P edge of the anion (computed length 2.810 Å) and displaying an unusually low P−H coupling of 4 Hz. A similar structure, with the agostic H atom replaced with SnH_3, was found to be a satisfactory model for the minor isomer of the tin compound and represents a third and unprecedented coordination mode of the diphosphorus ligand. The agostic complex undergoes a fluxional process involving the intermediacy of the nonagostic isomer $[Mo_2Cp_2(\mu\text{-}\kappa^2\text{:}\kappa^2\text{-}P_2H)(\mu\text{-}PCy_2)(CO)_2]$, which was computed to display a geometry comparable to the major isomers of the ER_3 compounds (P−P = 2.183 Å; P−P−H = 81.7°).

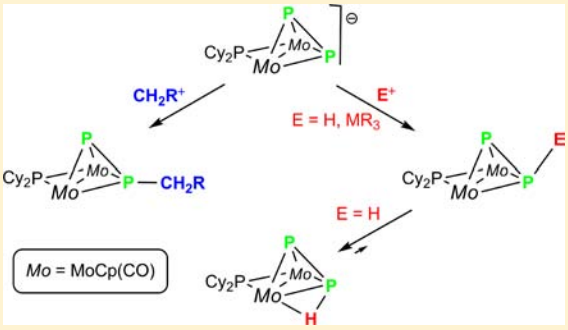

INTRODUCTION

White phosphorus (P_4) activation and functionalization has attracted much interest among inorganic chemists for more than 40 years.[1,2] Part of this interest stems from the convenience to replace our current industrial technology to produce organophosphorus derivatives, circumventing the use of environmentally hazardous and toxic chemicals such as chlorine gas. Many transition-metal complexes are known to activate this small molecule, to give products having new P_n-containing ligands (n = 1−24)[2,3] displaying very different coordination modes, and some functionalization studies have been also carried out.[2] Among all the reported ways to degrade the P_4 molecule, its symmetrical cleavage to give $\mu_2\text{-}\kappa^2\text{:}\kappa^2\text{-}P_2$ ligands is relatively well-precedented. The first example of this reaction was provided by Scherer and co-workers, reporting in 1984 that the triply bonded $[Mo_2Cp_2(CO)_4]$ would react with P_4 in refluxing toluene to give the dimolybdenum complex $[Mo_2Cp_2(CO)_4(\mu\text{-}\kappa^2\text{:}\kappa^2\text{-}P_2)]$.[4] There are, however, other routes to prepare these sorts of complexes having a M_2P_2 tetrahedral core. For instance, Markó and co-workers had reported a decade earlier the preparation of the related dicobalt complex $[Co_2(CO)_6(\mu\text{-}\kappa^2\text{:}\kappa^2\text{-}P_2)]$, the first example of these sorts of compounds, from the reaction of the metal carbonylate $Na[Co(CO)_4]$ with PX_3 (X = Cl or Br).[5]

Some reactivity studies have been also performed on these P_2-bridged complexes, mostly involving the addition of simple acceptor molecules, such as transition-metal fragments, these typically leaving an "intact" M_2P_2 core, although degradation, insertion, or bond cleavage reactions are also known.[2a,b] Concerning the first type of reactions, five different binding modes of the incoming fragment to the M_2P_2 unit have been reported so far in the literature (Chart 1). The "end-on" types (**I** and **II** in Chart 1) involve the binding of metal fragments (M′ in Chart 1) to one or both P atoms via the lone pairs (LP) of the latter and are exemplified by the addition of $[M'(CO)_5]$ fragments to $[M_2Cp_2(CO)_4(\mu\text{-}\kappa^2\text{:}\kappa^2\text{-}P_2)]$ complexes (M = Mo, W; M′ = Cr−W).[6] The "side-on" type (**III** in Chart 1) involves the attachment of the metal fragment at the P−P edge and has been found by Scheer and co-workers in self-assemblies based on $[Mo_2Cp_2(CO)_4(\mu\text{-}\kappa^2\text{:}\kappa^2\text{-}P_2)]$ and group 11 cations.[7] This alternative binding mode is actually reminiscent of the addition

Received: July 23, 2012
Published: September 24, 2012

   dx.doi.org/10.1021/ic301612g | *Inorg. Chem.* 2012, 51, 11061−11075

Chart 1

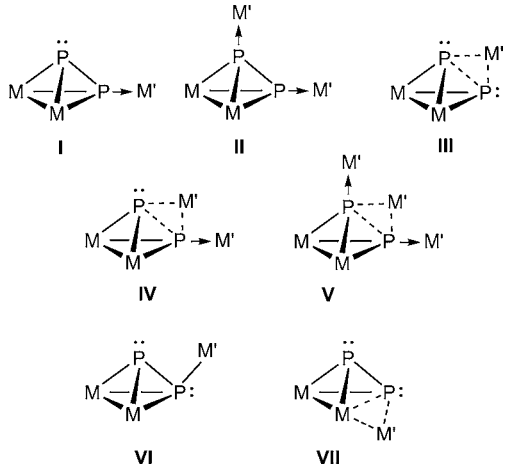

of the bare H^+ and Li^+ cations to the P_4 molecule, a reaction computed to take place preferentially at a P−P edge, rather than at a P vertex.[8] More recently, some complexes displaying "side-on"/"end-on" combinations (types **IV** and **V** in Chart 1) have been isolated from the reactions of $[Mo_2Cp_2(CO)_4(\mu\text{-}\kappa^2\text{:}\kappa^2\text{-}P_2)]$ with Cu(I) species in the presence of di- or triphosphines.[9]

Recently, we reported that the unsaturated anionic complex $[Mo_2Cp_2(\mu\text{-}PCy_2)(\mu\text{-}CO)_2]^-$ (**1**) was able to symmetrically cleave the P_4 molecule at room temperature to give the complex $[Mo_2Cp_2(\mu\text{-}PCy_2)(CO)_2(\mu\text{-}\kappa^2\text{:}\kappa^2\text{-}P_2)]^-$ (**2**),[10] the first anionic diphosphorus complex with a M_2P_2 tetrahedral core.[11] A preliminary exploration of its reactivity toward mild electrophiles revealed an unexpected dual donor ability of the P_2 unit involving the same P atom: (a) one involving the LP of that P atom, exemplified by the reaction with MeI to give the diphosphenyl complex $[Mo_2Cp_2(\mu\text{-}\kappa^2\text{:}\kappa^2\text{-}P_2Me)(\mu\text{-}PCy_2)(CO)_2]$ (P−P−C angle of ca. 122.8(1)°, binding mode of type **I**), and (b) a second one involving electron density located in a high-energy molecular orbital of **2** (and having both σ(Mo−P) and π(P−P) bonding character, according to density functional theory (DFT) calculations), exemplified by the reaction with $ClSnPh_3$ to give $[Mo_2Cp_2(\mu\text{-}\kappa^2\text{:}\kappa^2\text{-}P_2SnPh_3)(\mu\text{-}PCy_2)(CO)_2]$.[10] The latter represents a novel and unprecedented coordination mode of the M_2P_2 tetrahedral core (**VI** in Chart 1) in which the incoming electrophile is bound to one of the P atoms in a position intermediate between those implied by the "end-on" and "side-on" modes, geometrically identified by an acute P−P−M′ angle close to 90° (80.3(1)° in the mentioned tin compound). It was thus of interest to examine whether this was a rare, isolated example or indeed a new coordination mode to be found in the reactions of **2** with other electrophiles and to determine the chemical consequences (if any) of this unusual geometrical arrangement. In this paper we give a full account of our studies on the reactivity of the lithium salt of **2** toward electrophiles based on the group 14 elements, of general formula XER_3 (X = halogen; E = C, Si, Ge, Sn, Pb; R = H, alkyl or aryl). The bonding and dynamic behavior of some of these products has been also analyzed using DFT calculations. As it will be discussed, we have found that this novel coordination mode of the diphosphorus ligand is actually the preferred one when using most of the electrophiles analyzed and that a facile shift of the added electrophile between both P atoms of the diphosphorus ligand takes place in these cases. Moreover, we have also found that the Mo−P edge of the tetrahedral Mo_2P_2 core also is a competitive binding site for some of these electrophiles, even dominant in the case of the proton, this representing another unreported coordination mode of the diphosphorus ligand (**VII** in Chart 1). A fine balance between electronic and steric effects seems to determine the relative stability of the three types of derivatives of the diphosphorus complex **2**.

RESULTS AND DISCUSSION

Synthesis and Structural Characterization of the Anion 2. A freshly prepared tetrahydrofuran solution of the Li^+ salt of the unsaturated anion **1**[12] reacts with one equivalent of P_4 at room temperature to give solutions containing the Li^+ salt of the anionic diphosphorus complex **2** (**Li-2**) as the only organometallic product detectable by ^{31}P NMR spectroscopy. Although the composition of the product might suggest that only half a mole of P_4 would be enough for this reaction to be completed, careful experiments revealed that one mole of P_4 is consumed per mole of anion **1**. Unfortunately we could not establish the fate of the remaining "P_2" moiety because no other P-containing products were observed in the ^{31}P NMR spectrum of the crude reaction mixture.

The geometry of the anion **2** was optimized in our preliminary study (Figure 1 and Table 1),[10] using Density

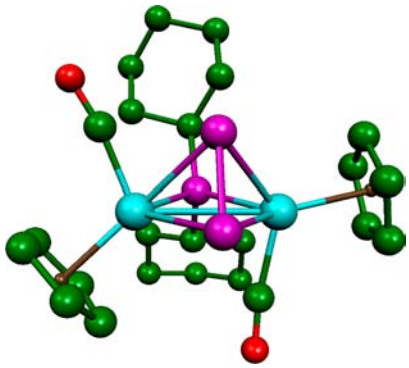

Figure 1. DFT-optimized structure of the anion **2**.[10]

Functional Theory (DFT) methods.[13] The molecule displays a Mo_2P_2 tetrahedral core, with a PCy_2 ligand symmetrically bridging the metal atoms in the same plane defined by one of the Mo_2P triangles, conventionally identified as the "base" of the tetrahedron. The coordination sphere of the metal atoms is completed by Cp and CO ligands in a somewhat distorted transoid arrangement, probably induced by the proximity of the "apical" phosphorus atom (P2 in Table 1). Thus, the CO ligand placed close to this atom is forced to point away from the intermetallic vector (Mo−Mo−C(O) = 112.0°), whereas the other one is slightly bent over the metal−metal bond (Mo−Mo−C(CO) 78.9°). This is a common structural motif found in dimolybdenum complexes of the type $[Mo_2Cp_2(\mu\text{-}PCy_2)(\mu\text{-}\kappa^2\text{:}\kappa^2\text{-L})(CO)_2]$ where L is a bidentate five-electron donor ligand such as formimidoyl,[14] carboxylate-alkenyl,[15] or chalcoacyl,[16] and it is also observed for all derivatives of **2** to be discussed below.

The computed intermetallic distance of 3.025 Å is consistent with the presence of a single Mo−Mo bond as required by the EAN formalism and actually is quite similar to that measured for the tetracarbonyl complex $[Mo_2Cp_2(CO)_4(\mu\text{-}\kappa^2\text{:}\kappa^2\text{-}P_2)]$

dx.doi.org/10.1021/ic301612g | Inorg. Chem. 2012, 51, 11061−11075

Table 1. Selected Bond Lengths (Å) and Angles (deg) for Compounds 2, 3a, 5, 6, and A[a]

parameters	**2**[10]	**3a**[10]	**5**	**6**[10]	**A**
Mo1−Mo2	3.025	3.0172(4)	2.9823(3)	2.9860(7)	3.051
Mo1−P1	2.456	2.458(1)	2.4525(7)	2.445(1)	2.504
Mo2−P1	2.457	2.432(1)	2.4239(7)	2.416(1)	2.485
Mo1−P2	2.565	2.542(1)	2.4497(7)	2.442(2)	2.460
Mo2−P2	2.528	2.521(1)	2.4265(6)	2.420(2)	2.436
Mo1−P3	2.572	2.413(1)	2.4718(7)	2.489(2)	2.538
Mo2−P3	2.573	2.399(1)	2.4931(7)	2.498(2)	2.566
P2−P3	2.095	2.085(1)	2.1749(9)	2.201(2)	2.183
P3−E	-	1.827(3)	2.3388(7)	2.533(2)	1.435
P2−P3−E	-	122.8(1)	86.7(1)	80.3(1)	81.7
Mo2−Mo1−C1	112.0	115.4(1)	117.7(1)	115.0(2)	117.2
Mo1−Mo2−C2	78.9	79.8(1)	78.5(1)	79.1(2)	79.3

[a]Values according to the labeling of the scheme shown below. Data for **2** and $[Mo_2Cp_2(\mu\text{-}\kappa^2\text{:}\kappa^2\text{-}P_2H)(\mu\text{-}PCy_2)(CO)_2]$ (isomer **A** of compound **4**, see text) are for the DFT-optimized structures.

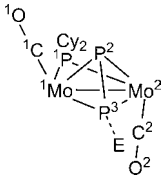

Table 2. Selected IR and $^{31}P\{^1H\}$ NMR Data at 295 K for New Compounds

compound	ν(CO)[a]	δ_P (J_{PP})[b]		
		μ-PCy_2	$P^{ap}(P_2)$	$P^{bs}(P_2)$
$Li[Mo_2Cp_2(\mu\text{-}PCy_2)(CO)_2(\mu\text{-}\kappa^2\text{:}\kappa^2\text{-}P_2)]$ (**Li-2**)	1837 (vs), 1770 (w), 1669 (s)[c,d]	165.3 (br)[e]	−80.0 (br)[e]	−273.0 (br)[e]
$[(PPh_3)_2N][Mo_2Cp_2(\mu\text{-}PCy_2)(CO)_2(\mu\text{-}\kappa^2\text{:}\kappa^2\text{-}P_2)]$ (**PPN-2**)	1819 (s), 1767 (vs)[c,d]	155 (vbr)[f]	−165 (vbr)[f]	
$[Li(C_8H_{16}O_4)_2][Mo_2Cp_2(\mu\text{-}PCy_2)(CO)_2(\mu\text{-}\kappa^2\text{:}\kappa^2\text{-}P_2)]$ ([**Li(12-crown-4)$_2$**]-**2**)	1827 (vs), 1763 (s)[c,d]	163.8 (br)[f]	−170.2 (br)[f]	
$[Mo_2Cp_2(\mu\text{-}\kappa^2\text{:}\kappa^2\text{-}P_2Me)(\mu\text{-}PCy_2)(CO)_2]$ (**3a**)	1874 (m), 1823 (vs)	156.9 (16, 13)	−293.2 (503, 13)	− 84.3 (503, 16)
$[Mo_2Cp_2(\mu\text{-}\kappa^2\text{:}\kappa^2\text{-}P_2CH_2Ph)(\mu\text{-}PCy_2)(CO)_2]$ (**3b**)	1874 (m), 1823 (vs)	156.5 (16, 15)	−279.2 (497, 15)	−48.1 (497, 16)
$[Mo_2Cp_2(\mu\text{-}\kappa^2\text{:}\kappa^1,\eta^2\text{-}HP_2)(\mu\text{-}PCy_2)(CO)_2]$ (**4**)	1890 (w), 1863 (vs)[c]	141.8[g]	−127.9 (461)[g]	−312.9 (461)[g]
$[Mo_2Cp_2(\mu\text{-}\kappa^2\text{:}\kappa^2\text{-}P_2GePh_3)(\mu\text{-}PCy_2)(CO)_2]$ (**5**)	1872 (s, sh), 1841 (vs)	143.7 (6)	−155 (br)	
$[Mo_2Cp_2(\mu\text{-}\kappa^2\text{:}\kappa^2\text{-}P_2SnPh_3)(\mu\text{-}PCy_2)(CO)_2]$ (**6**)	1875 (s, sh), 1850 (vs)	140.3[h] [43][i]	−148.0 (br)[h]	
$[Mo_2Cp_2(\mu\text{-}\kappa^2\text{:}\kappa^2\text{-}P_2PbPh_3)(\mu\text{-}PCy_2)(CO)_2]$ (**7**)	1875 (s), 1848 (vs)	142.0 (br)	−107.7 (br)	
$[Mo_2Cp_2(\mu\text{-}\kappa^2\text{:}\kappa^2\text{-}P_2PbMe_3)(\mu\text{-}PCy_2)(CO)_2]$ (**8**)	1865 (vs), 1828 (s)	141.8 (br)[g]	−132.5 (br)[g]	

[a]Recorded in dichloromethane solution, with C−O stretching bands [ν(CO)] in cm^{-1}. [b]Recorded in CD_2Cl_2 at 121.50 MHz and 298 K, with coupling constants (J_{PP}) in Hz; P^{ap} and P^{bs} refer respectively to the "apical" and "basal" P atoms of the Mo_2P_2 tetrahedron (see text). [c]Recorded in tetrahydrofuran solution. [d]A band of variable intensity at 1866 cm^{-1} was always observed, attributed to partial oxidation of the anion within the CaF_2 plates during recording of the spectra. [e]Recorded in a tetrahydrofuran/C_6D_6 mixture (10:1) at 163 K; just a broad resonance at −166.4 ppm was observed for the P_2 ligand at 293 K. [f]Recorded in tetrahydrofuran with a D_2O insert. [g]Recorded in toluene-d_8 at 161.97 MHz. [h]Recorded at 161.97 MHz. [i]$J(^{31}P-^{117/119}Sn)$.

(3.0206(4) Å).[4] In the same vein, the P−P distance in **2** (2.095 Å) is also similar to that in the latter diphosphorus complex (2.079(2) Å)[4] and ca. 0.12 Å shorter than the interatomic separation in the P_4 molecule (2.21 Å). This might be indicative of the presence of some π(P−P) bonding character in that bond, a matter to be discussed below. Although the P_2 ligand in **2** is almost symmetrically bridging the bimetallic center, as denoted by the similar P−Mo1/Mo2 distances, the P atoms have quite different chemical environments, even if the Mo−P lengths are comparable to each other. This constitutes a substantial difference when comparing **2** to the extensively studied $[Mo_2Cp_2(CO)_4(\mu\text{-}\kappa^2\text{:}\kappa^2\text{-}P_2)]$, the latter displaying equivalent environments for the P atoms of the P_2 ligand. As a result, the reactivity of **2** is more intensely located at the "basal" P atom of its diphosphorus ligand.

The IR spectrum in tetrahydrofuran solution for the lithium salt of **2** displays three C−O stretching bands at 1837 (vs), 1770 (w), and 1669 (s) cm^{-1} (Table 1), this suggesting the presence of tight Mo−CO···Li^+ ion pairs in equilibrium with the solvent-separated ions, a typical situation in the alkaline salts of transition-metal carbonylates.[17] In order to assign the stretching bands corresponding to both types of species, the lithium cation was "sequestered" by the progressive addition of 12-crown-4 (up to 16 equivalents) to tetrahydrofuran solutions of **Li-2**, this eventually leading to the complete disappearance of the band at 1669 cm^{-1}, to leave an IR spectrum with just two strong C−O stretches at 1827 and 1763 cm^{-1} that can be safely assigned to the "free" anion of the salt [**Li(12-crown-4)$_2$**]-**2**, comparable to the solvent-separated anion in **Li-2**. A similar IR spectrum was obtained when adding one equivalent of [PPN]Cl (PPN = $[(Ph_3P)_2N]^+$) to a tetrahydrofuran solution of **Li-2**, this yielding **PPN-2** having a solvent-separated anion with stretching bands at 1819 (s) and 1767 (vs) cm^{-1}. We note that all these data are consistent with the DFT-computed C−O

dx.doi.org/10.1021/ic301612g | Inorg. Chem. 2012, 51, 11061−11075

stretches for the anion **2** in the gas phase (1911 and 1889 cm^{-1}, with 43:100 relative intensities), after allowing for the 5−10% overestimation usually found for DFT-derived IR data.[18] Eventually, the above experiments allow us to safely assign the band at 1669 cm^{-1} of **Li-2** to the C−O stretch of the carbonyl ligand in a tight ion pair of the type Mo−CO···Li^+, whereas the band at 1837 cm^{-1} would be mainly due to the stretch of the other CO ligand in this species. Therefore, the weak band at 1770 cm^{-1} for **Li-2** is assigned to the asymmetric C−O stretch of the solvent-separated anion, present only in small amounts. This minor species should also give rise to a symmetrical stretch at ca. 1825 cm^{-1}, obviously masked by that of the dominant tight ion pair. We finally note that the C−O stretching frequency of the carbonyl involved in the strong Mo−CO···Li^+ interaction (1669 cm^{-1}) is comparable to that measured for the ion-paired carbonyl in $Li[FeCp(CO)(PPh_3)]$ (1710 cm^{-1}).[19]

The $^{31}P\{^1H\}$NMR spectrum of **Li-2** at 298 K in tetrahydrofuran/C_6D_6 (10/1) displays two broad resonances at 166.7 and −166.4 ppm, corresponding to the PCy_2 and P_2 ligands, respectively, this being indicative of the occurrence of a dynamic process averaging the inequivalent environments of the nuclei of the diphosphorus ligand. Similar spectra were recorded for the solvent-separated salts [**Li(12-crown-4)$_2$**]-**2** and **PPN-2** (Table 2). Upon cooling down to 163 K, the more shielded resonance of **Li-2** splits into two broad signals at −80.0 and −273.0 ppm, that we can assign to the apical and basal P atoms, respectively, on the basis of the relative values of the DFT-computed chemical shifts for **2** (Table 3).

To account for the above observations we propose the occurrence in solution of the fluxional process depicted in Scheme 1, involving a swing of the P_2 group around the Mo−Mo axis, concerted with some rearrangement of the Cp and CO ligands (not shown in the scheme) so as to fully exchange the chemical environments of the pairs of Cp, CO, and $P(P_2)$ donor centers. The coalescence temperature was roughly measured to be 183 ± 5 K, which allows us to estimate an energy barrier for this process ($\Delta G^{\#}_{183}$) of 26 ± 1 kJ/mol.[20]

Table 3. Computed NMR Parameters for Compounds 2−6[a]

parameter	2	3a	4	6	A
σ^d (P1)	970.1	971.2	971.1	977.4	970.7
σ^d (P2)	976.4	976.7	976.5	985.6	978.1
σ^d (P3)	976.5	978.7	974.8	987.4	974.4
σ^p (P1)	−903.1	−890.0	−880.5	−878.4	−848.3
σ^p (P2)	−710.1	−454.3	−657.1	−796.4	−1086.0
σ^p (P3)	−496.2	−651.7	−348.5	−409.9	−345.6
σ (P1)	67.0	81.2	90.7	99.0	122.4
σ (P2)	266.3	522.4	319.4	189.2	−107.9
σ (P3)	480.3	327.0	626.3	577.4	628.8
δ (P1)	171.2	156.9	147.5	139.1	115.7
δ (P2)	−28.2	−284.3	−81.3	49.0	346.0
δ (P3)	−242.2	−88.9	−388.2	−339.3	−390.7
J(P3−H)			−9[b]		132
J(P3−P2)			−506		−199

[a]Values in ppm for the DFT-optimized structures, with the labeling scheme shown below; see the Experimental Section for details. σ^d and σ^p stand respectively for the diamagnetic and paramagnetic contributions to the magnetic shielding (σ) of the P atoms. Chemical shifts (δ) are given so as to fit the computed value of δ(P1) of compound **3a** to the experimental figure of 156.9 ppm, and coupling constants (J) are given in hertz.

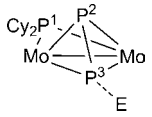

[b]J(H−P2) = −1; J(H−P1) = 2.

Scheme 1. [*Mo* = MoCp(CO)]

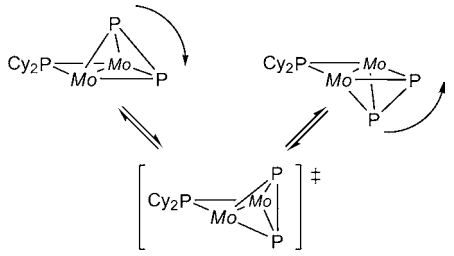

Reactivity of 2 Toward Group 14 Electrophiles. Freshly prepared solutions of **Li-2** reacted rapidly at room temperature with different electrophiles based on the group 14 elements (E) of the type XER_3 (X = halogen), although the structure and nature of the products was strongly dependent on the particular element involved. The reactions with the C-based electrophiles MeI or $ClCH_2Ph$ proceeded with good selectivity at room temperature to give the corresponding diphosphenyl complexes $[Mo_2Cp_2(\mu\text{-}\kappa^2\text{:}\kappa^2\text{-}P_2CH_2R)(\mu\text{-}PCy_2)(CO)_2]$ (R = H (**3a**), Ph (**3b**)) after 5 min or 3 h, respectively (Scheme 2). To our knowledge, these are the first examples of complexes with diphosphenyl ligands in a $\mu_2\text{-}\kappa^2\text{:}\kappa^2$ coordination mode.[21] In contrast, the reaction of **2** with $BrSiMe_3$ did not lead to the expected silyldiphosphenyl product but yielded instead the agostic diphosphenyl complex $[Mo_2Cp_2(\mu\text{-}\kappa^2\text{:}\kappa^1,\eta^2\text{-}HP_2)(\mu\text{-}PCy_2)(CO)_2]$ (**4**), formally derived from the attachment of a proton to one of the basal Mo−P edges of the anion **2**. We assume that an undetected silyldiphosphenyl complex $[Mo_2Cp_2(\mu\text{-}\kappa^2\text{:}\kappa^2\text{-}P_2SiMe_3)(\mu\text{-}PCy_2)(CO)_2]$ would be first formed in this reaction, it rapidly reacting with trace amounts of water present in the solution, thus accomplishing a rapid hydrolysis of the newly formed P−Si bond to give the final

Scheme 2

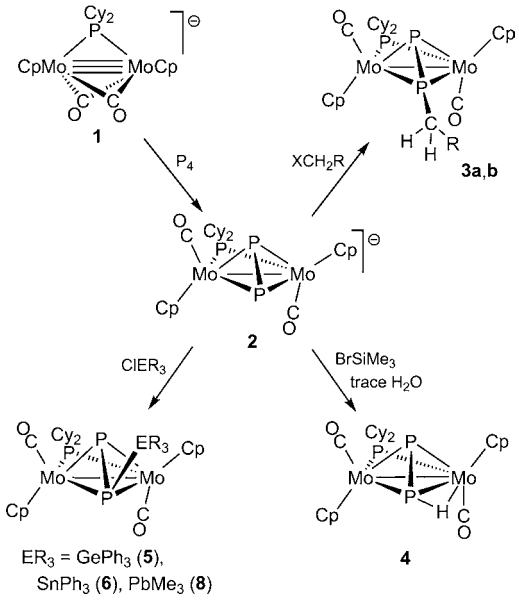

dx.doi.org/10.1021/ic301612g | Inorg. Chem. 2012, 51, 11061−11075

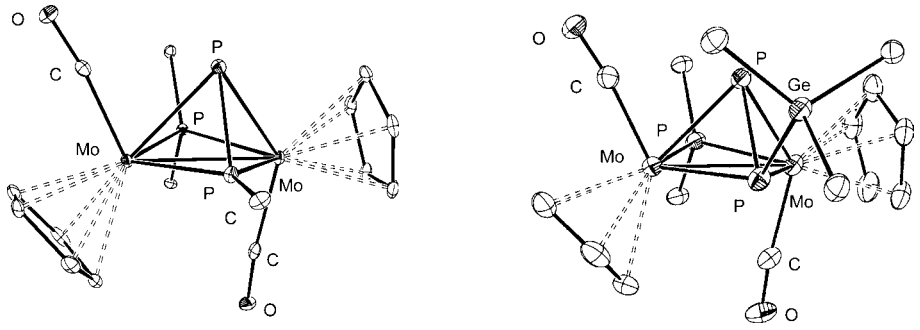

Figure 2. ORTEP diagram (30% probability) of compounds **3a** (left)[10] and **5** (right) with H atoms, Cy and Ph groups (except the C^1 atoms) omitted for clarity.

product and some siloxane byproduct. Compound **4** can be also obtained by direct protonation of **2** with a source of protons such as $[NH_4][PF_6]$, although the yield is much lower because of the complex mixture of products generated in the latter reaction. An interesting question emerges from the above results, namely whether a nonagostic diphosphenyl complex $[Mo_2Cp_2(\mu\text{-}\kappa^2\text{:}\kappa^2\text{-}P_2H)(\mu\text{-}PCy_2)(CO)_2]$ (**A**) is involved in the above reactions leading to the agostic complex **4**. That would not be surprising, since the hydrolysis of P−Si bonds is a well established methodology to generate P−H bonds.[2e] As it will be discussed later on, the isomer **A** of compound **4** was computed to be less stable than the agostic structure by some 29 kJ/mol, and it plays an active role in the solution dynamics of this agostic complex. We should note that **4** appears to be the first reported diphosphenyl complex displaying an agostic M−H−P interaction, with its closest precedent being found in the cation $[Co(HP_3)(triphos)]^+$ reported by Stoppioni and coworkers, presumably having a hydrogen atom bridging one of the Co−P edges of the CoP_3 tetrahedron.[22]

The reaction of **Li-2** with organo-chlorides of the heavier elements of the group 14 (Ge, Sn, Pb) gave the corresponding diphosphenyl-like complexes of the general formula $[Mo_2Cp_2(\mu\text{-}\kappa^2\text{:}\kappa^2\text{-}P_2ER_3)(\mu\text{-}PCy_2)(CO)_2]$ (ER_3 = $GePh_3$ (**5**), $SnPh_3$ (**6**), $PbPh_3$ (**7**), $PbMe_3$ (**8**)). Some of these products were found to display in solution a mixture of two (**5** and **6**) or three (**7**) isomers and have unusual structural features to be discussed next.

We should finally note that small amounts (ca. 10−20%) of a yellow side-product were formed in all of the above reactions, as deduced from the chromatographic workup of the corresponding reaction mixtures. Such a product, apparently common to all these reactions, might arise from a side electron-transfer pathway competing with the main, acid−base reaction. Unfortunately we have not been able to properly isolate and characterize this neutral product, which seems to be NMR-silent and gives rise to a somewhat broad C−O stretching band at 1864 cm^{-1} in dichloromethane solution, not far from those of the diphosphenyl complexes **3**.

Solid-State Structure of Compounds 3a, 5, and 6. The structures of compounds **3a** and **6** were determined in our preliminary study on this chemistry,[10] and we have now determined the structure of the germanium compound **5** (Figure 2). The most relevant geometrical parameters of all these compounds are collected in Table 1, along with the DFT-computed parameters for the anion **2** and the nonagostic isomer **A** of the diphosphenyl complex **4**. We note that the geometrical parameters of the DFT-computed structures of the complexes **3a** and **6** were in good agreement with the experimental values,[10] with the computed lengths involving the metal atoms being slightly longer (by less than 0.05 Å) than the corresponding experimental data, as usually found with the functionals currently used in the DFT computations of transition-metal complexes.[13a,23]

The structures of the neutral complexes are quite similar to the structure computed for the anion **2**, except for the position of the added electrophile (Me, $GePh_3$, $SnPh_3$, H) attached to the basal P atom of the P_2 ligand. In the case of the methyl derivative **3a**, the latter moiety defines an angle with the P−P bond of 122.8(1)° (computed 121.1°), only slightly smaller than those found for the diphosphene compound $[Fe_2(CO)_6(\mu\text{-}\kappa^2\text{:}\kappa^2\text{-}P_2{}^tBu_2)]$ (average angle of ca. 131°).[24] Accordingly, this structure can be classified within the common type **I** (Chart 1). In contrast, for the other three compounds the incorporated electrophile defines a much lower P−P−E angle, in the range 80−87°, and must be classified into an entirely new class of diphosphorus complexes (type **VI**). The P−P and Mo−P bonds within the Mo_2P_2 tetrahedron are differently modified (with respect to the values in the anion **2**) in these two classes of structures. Thus, the P−P distance in **3a** (2.085(1) Å) is very similar to the one computed for the anion, whereas the corresponding values for compounds **5**, **6**, and **A** are ca. 0.1 Å longer. As for the Mo−P lengths, those in the methyldiphosphenyl complex **3a** involving the basal P atom become shorter (by ca. 0.12 Å) than those involving the apical P atom, but the reverse applies for compounds **5**, **6**, and **A**, although the differences here are smaller (0.05−0.1 Å). We note that these metric parameters are consistent with the different orbital interactions involved in both classes of compounds, to be discussed later on.

Solution Structure of Compounds 3a,b. The spectroscopic data in solution for these diphosphenyl complexes are similar to each other and consistent with the solid-state structure of **3a** discussed above. Both compounds display identical C−O stretching bands at 1874 (m) and 1823 (vs) cm^{-1}, with a pattern consistent with a distorted transoid arrangement of the $M_2(CO)_2$ oscillator.[25] Their $^{31}P\{^1H\}$ NMR spectra exhibit three distinct resonances, attributed respectively to the PCy_2 (ca. 157 ppm), basal PR (ca. −70 ppm), and apical P (ca. −290 ppm) donors. The assignment of the diphosphenyl resonances was confirmed with a H-coupled ^{31}P NMR spectrum of **3a**, this showing an unresolved H-coupling only to the resonance at −84.3 ppm, and moreover it is consistent with the chemical shifts computed for the DFT-optimized structure of **3a** (Table 3). The P atoms of the diphosphenyl ligand show a large mutual coupling of ca. 500 Hz, a value typical of directly bound P−P atoms with some π interaction, it

dx.doi.org/10.1021/ic301612g | Inorg. Chem. 2012, 51, 11061−11075

being reminiscent of the values found for free and κ^1-bound diphosphene compounds.[21] This observation is also consistent with the short P−P distance found in the solid state for **3a** (ca. 0.13 Å shorter than the reference single P−P bond length).

Solution Structure of Compound 4. The IR spectrum of **4** in solution displays two C−O stretches with relative intensities (w and vs, in order of decreasing frequencies) indicative of a transoid arrangement of the carbonyls, with frequencies ca. 30 cm^{-1} higher than those of compounds **3**. The presence of a hydrogen atom in the vicinity of the metal atoms was unequivocally revealed by the appearance of a strongly shielded doublet resonance (J_{PH} = 8 Hz) at −10.05 ppm in the ^{1}H NMR spectrum. This chemical shift is somewhat higher than the typical values observed for bridging hydrides in related dimolybdenum complexes (ca. −13 ppm for $[Mo_2Cp_2(\mu\text{-}H)(\mu\text{-}PRR')(CO)_4]$)[26] and might be itself consistent with the presence of a terminal, rather than bridging, hydride. Indeed, DFT calculations of likely structures revealed that an H-bridged structure (**E**) would be some 50 kJ/mol less stable than any of the four possible isomers with terminal hydrides (Figure 3 and

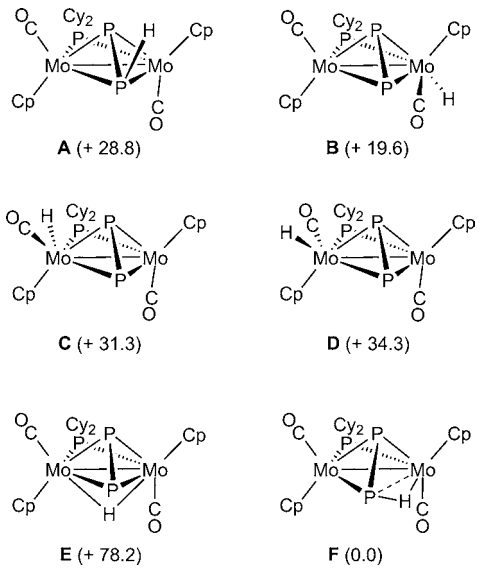

Figure 3. DFT-computed Gibbs free energies (kJ/mol) for different isomers of compound **4**.

Supporting Information). Among the latter, the most stable was the one with the hydride ligand *trans* to the apical atom and *cis* to the PCy_2 ligand (**B**), while the one with the hydride ligand *trans* to both the apical P atom and the PCy_2 ligand was not a minimum in the potential energy surface but instead its H atom converged into a bridging position between the Mo and P atoms (interaction of type **VII** in Chart 1). The resulting molecule **F** effectively displays a diphosphenyl ligand with an agostic P−H−Mo interaction (P−H = 1.566, H−Mo = 1.918 Å), a quite elongated P−Mo bond (2.810 Å), and a relatively short P−P bond (2.128 Å). Surprisingly, the computed energy for the agostic isomer **F** was some 20 kJ/mol lower than any of the hydride isomers and 29 kJ/mol lower than its nonagostic diphosphenyl isomer **A** (a structure of type **VI**, and not of type **I**, a matter to be discussed latter on); therefore, the agostic structure must be taken as the ground state of compound **4** (Figure 4). Indeed, this structure was the only one leading to computed relative intensities for the symmetric and asymmetric C−O stretches (ca. 20/120) qualitatively comparable to the

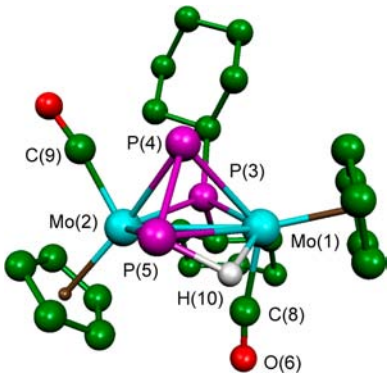

Figure 4. DFT-optimized structure for the agostic complex **4** (structure **F**) with hydrogen atoms, except H10, omitted for clarity. Selected bond lengths (Å) and angles (deg): Mo1−Mo2 = 3.000, P4−P5 = 2.128, Mo1−P3 = 2.502, Mo2−P3 = 2.471, Mo1−P4 = 2.517, Mo2−P4 = 2.562, Mo1−P5 = 2.810, Mo2−P5 = 2.523, Mo1−H10 = 1.918, P5−H10 = 1.566; Mo2−Mo1−C8 = 78.2, Mo1−Mo2−C9 = 118.3, P4−P5−H10 = 96.3.

experimental intensities of compound **4** (Table 2), whereas the hydride structures **B**, **C**, and **D** led to relative intensities less consistent or inconsistent with the experimental spectrum (ca. 50/100, 80/70, and 75/75, respectively).

The computed ^{31}P NMR parameters for the structure **F** (entry **4** in Table 3) are not very different from those of the anion **2**, therefore allowing the assignment of the most shielded resonance of the HP_2 ligand in **4** (−312.9 ppm) to the basal P atom, and the less shielded one (−127.9 ppm) to the apical P atom. We note that the PP coupling in **4** remains very high (461 Hz), indicating the retention of a strong bonding interaction, as found in the anion **2** and in the alkyldiphosphenyl derivatives **3**. This is consistent with the relatively short P−P length computed for the structure **F** and in excellent agreement with the computed figure of −506 Hz for this coupling. The negative value of this figure can be attributed to the influence of the electron LPs present at each of the P atoms, not involved in bonding with the H atom.[27]

The room temperature ^{1}H NMR spectrum of **4** displays a broad resonance at 4.72 ppm ($\Delta\nu_{1/2}$ = 16 Hz at 298 K) corresponding to the inequivalent Cp ligands, which is indicative of the occurrence of a dynamic process in solution. At 258 K the spectrum already displays well separated Cp resonances at 4.71 and 4.59 ppm consistent with the static structure, while the agostic H resonance now displays coupling to all three P atoms (8.8, 4.4, and 3.4 Hz) which could be safely assigned, on the basis of selective ^{31}P decoupling experiments, to the PCy_2, basal, and apical diphosphenyl atoms, respectively. Since the small couplings vanish in the room temperature spectrum, we must conclude that they are opposite in sign (−4.4 and +3.4 Hz), so as to yield an averaged value close to zero. Moreover, from the coalescence temperature of the Cp resonances (294 K at 400.13 MHz) we can estimate a Gibbs free energy of $\Delta G^{\#}_{294}$ = 60.5 ± 0.5 kJ/mol for the kinetic barrier of the corresponding fluxional process,[21] which is ca. 34 kJ/mol higher than that measured for the anion **2** at 183 K. A proposal for such a process will be discussed later on.

A puzzling spectroscopic feature of the agostic complex **4** is that it displays a very low P−H coupling of ca. 4 Hz, much below the values previously measured for agostic P−H−M interactions in protonated PR_2-bridged complexes (half the values of the corresponding nonagostic H−P couplings or

dx.doi.org/10.1021/ic301612g | *Inorg. Chem.* 2012, 51, 11061−11075

Table 4. Selected $^{31}P\{^1H\}$ NMR Data at 178 K for Compounds 5−8

	isomer VI δ_P (J_{PP})[a]			isomer VII δ_P (J_{PP})[a]		
compound	μ-PCy_2	$P^{ap}(P_2)$	$P^{bs}(P_2)$	μ-PCy_2	$P^{ap}(P_2)$	$P^{bs}(P_2)$
5 (E = $GePh_3$)	138.6	27.5 (280)	−315.5 (280)	-	-	-
6 (E = $SnPh_3$)	139.3	38.8 (185)	−341.4 (185) [950][b]	143.5	−92.5 (475)	−239.6 (475)
7 (E = $PbPh_3$)[c]	213.5	57.7 (200)	−279 (br)	139.5	−46.5 (470)	−127.7 (470)
8 (E = $PbMe_3$)	139.0[d]	38.3 (220)[d]	−317.6 (220)[d] [1740][e]	-	-	-

[a]Recorded in CD_2Cl_2 solution at 161.97 MHz, with coupling constants (J) given in Hz; P^{bs} and P^{ap} refer respectively to the "basal" and "apical" P atoms of the Mo_2P_2 tetrahedron (see text). [b]$^1J(^{31}P-^{117/119}Sn)$. [c]The isomer of type **VI** for this compound appears to have a cisoid arrangement of the MoCp(CO) fragments; moreover, a third isomer of unknown structure was detected at this temperature (see text). [d]In toluene-d_8 solution. [e]$^1J(^{31}P-^{207}Pb)$.

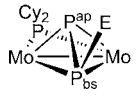

Isomer VI

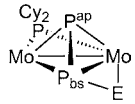

Isomer VII

above 100 Hz).[28] By considering that one-bond P−H couplings in nonagostic low-valent H_xP_n ligands are relatively low (100−200 Hz),[2e] we still might expect a P−H coupling above 50 Hz for **4**. Unfortunately, no P−H coupling could be measured for the only other related agostic complex reported previously ($[Co(HP_3)(triphos)]^+$) which, however, gave a comparably shielded resonance (−13.7 ppm).[22] Yet, the computed value for this coupling in **4** (−9 Hz) is in excellent agreement with the experimental value. It is tempting to propose the mentioned negative contribution of the LP at phosphorus to its one bond couplings as a likely cause of the anomalously low P−H coupling in this agostic complex. In any case, this effect means that it might be difficult in general to distinguish between alternative formulations of the type hydride $[L_nMH(P_x)]$ vs agostic $[L_nM(HP_x)]$ on the basis of the ^1H NMR data only since, as we now have shown, the agostic M−H−P interaction can lead to ^1H chemical shifts and H−P couplings very similar to the values expected for the corresponding hydride isomers. This circumstance should be taken into account in future studies on the hydrogenation of polyphosphorus ligands in the vicinity of transition-metal centers.

Solution Structure of Compounds 5, 6, and 8: Type VI vs Type VII Isomers. The spectroscopic data in solution for these compounds (Tables 2 and 4) are comparable to each other and in reasonable agreement with the solid-state structures of the germanium and tin compounds discussed above. The latter compounds display C−O stretching bands with a pattern consistent with a distorted transoid arrangement of the carbonyl ligands, but the intensities for the lead compound **8** are comparable to each other, this perhaps indicating a more distorted geometry in solution, with CO ligands positioned at almost right angles.[25] The NMR data, however, revealed dynamic behavior for all three compounds, because in each case a single and broad ^1H NMR resonance was observed for the inequivalent Cp groups, while the inequivalent atoms of the diphosphorus ligand also gave rise to a single and broad resonance in the range −155 to −108 ppm (Table 2).

Upon decreasing the temperature, all these averaged resonances eventually split into two of equal intensity in each case, in agreement with the solid-state structures (structure of type **VI**). The diphosphorus resonances now appear as doublets at very different chemical shifts, ca. 30 to 40 ppm and ca. −315 to −340 ppm (Table 4). The most shielded resonances can be safely assigned to the basal P atoms since they exhibit satellite lines displaying large couplings to either the $^{119/117}Sn$ or the ^{207}Pb nuclei of ca. 950 Hz (**6**) and 1740 Hz (**8**), these values being indicative of one-bond P−E couplings to these nuclei.[29,30] Moreover, the computed shifts for the DFT-optimized structure of **6** leads to the same assignment (Table 3), which turns out to be reversed with respect to the assignment in the diphosphenyl complexes **3** (strong deshielding for the basal P atom). A second and relevant spectroscopic feature is that the P−P coupling in these compounds (185 to 280 Hz, Table 4) takes almost half the values observed for the diphosphenyl complexes **3**, a clear reflection of the significant elongation operated on the corresponding P−P bonds, already noted, now approaching the conventional single-bond lengths and couplings.

At 178 K, the ^{31}P NMR spectra of **5** and **6** denoted the presence of very small amounts of a second species in each case, presumably an isomer of the main product. In the case of the germanium compound, this second isomer appears in a 1:13 ratio and gives rise to broad diphosphorus resonances at +7 and −299 ppm, not far from those of the main isomer, and is thus tentatively identified as a minor rotamer of compound **5** (rotation around the Ge−P bond may have been slowed down enough at that temperature to give observable rotamers). The second isomer for the tin compound appears in a 1:9 ratio but now gives rise to NMR resonances for the diphosphorus ligand quite different from those of the main isomer (−92.5 and −239.6 ppm, Table 4), and being strongly coupled to each other (J_{PP} = 475 Hz), as observed for compounds **3** or **4**. Structures containing $SnPh_3$ groups terminally bound to the Mo atoms are disfavored here due to the strong steric repulsions that would be induced by the bulky $SnPh_3$ group thus bound to the Mo_2 center. On the other hand, structures of type **I** (as those of compounds **3**), with $SnPh_3$ or SnH_3 groups end-on bound to the basal P atom, were not a minimum in the corresponding potential energy surfaces according to DFT calculations but converged into the structures of type **VI** already computed for the major isomer of **6** and its SnH_3 analogue (**6-H**), and the same was observed for a SnH_3 group placed at the apical P atom. However, a calculation of a SnH_3 analogue of the agostic complex **4** (that is, with a structure of type **VII**, Figure 5), gave a minimized structure with a Gibbs free energy only 14.2 kJ/mol above that of the major isomer of type **VI**, and thus must be taken as the most sensible proposal for the observed minor isomer of **6**. Note that the computed P−P length in this model complex is as short as that in the

dx.doi.org/10.1021/ic301612g | Inorg. Chem. 2012, 51, 11061−11075

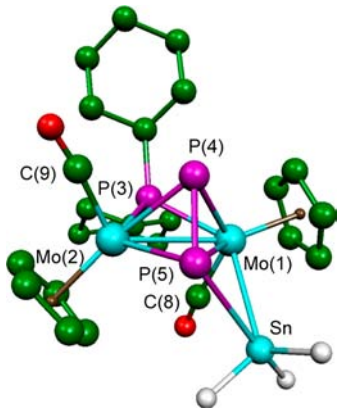

Figure 5. DFT-optimized structure for $[Mo_2SnH_3Cp_2(\mu_3\text{-}\kappa^2\text{:}\kappa^1\text{-}P_2)(\mu\text{-}PCy_2)(CO)_2]$ (**6-H**, isomer **VII**) with hydrogen atoms, except those bound to Sn, omitted for clarity. Selected bond lengths (Å) and angles (deg): Mo1−Mo2 = 3.060, P4−P5 = 2.083, Mo1−P3 = 2.574, Mo2−P3 = 2.451, Mo1−P4 = 2.555, Mo2−P4 = 2.555, Mo1−P5 = 2.754, Mo2−P5 = 2.507, Mo1−Sn = 2.927, P5−Sn = 2.892; Mo2−Mo1−C8 = 79.1, Mo1−Mo2−C9 = 120.1.

anion **2** and in any case consistent with the large experimental coupling of 475 Hz (Table 4). This molecule can be viewed as resulting from the 3c-2e interaction following the attachment of a SnH_3^+ cation to a basal Mo−P bond in the anion: accordingly, the interatomic distances within the Mo−P−Sn triangle are expected to be longer than the corresponding single-bond lengths. Indeed the computed Mo1−P5 length in the isomer **VII** of **6-H** is enlarged by some 0.25 Å, while the Mo1−Sn length of 2.927 Å is almost identical to that measured for $[Mo_2Cp_2(\mu\text{-}SnPh_3)(\mu\text{-}PCy_2)(CO)_2]$, with a $SnPh_3$ group bridging two Mo atoms (Mo−Sn ca. 2.92 Å), and significantly longer than the value expected for a 2c-2e single Mo−Sn bond in this sort of complexes (cf. 2.826(1) Å for $[Mo_2Cp_2(SnPh_3)(\mu\text{-}PCy_2)(CO)_4]$).[31] Finally, the P5−Sn length of 2.892 Å is ca. 0.3 Å longer than the corresponding lengths computed for the type **VI** isomers of **6** and **6-H** (ca. 2.54 A)[10] or those measured in the few triorganostannylphosphines structurally characterized so far (ca. 2.54 Å).[32]

Solution Structure of Compound 7. Although the room temperature IR and NMR spectra of the triphenyllead compound **7** were comparable to those of its germanium and tin analogues **5** and **6** (Table 2), the variable-temperature NMR spectra indicated a more complex situation, revealing the presence of up to three different interconverting isomers, these appearing in comparable amounts at 178 K (see the Experimental Section). Although the different coalescences were ill-defined, it seems that not only each isomer is fluxional but also that the interconversions between them are slower than the fluxional process within each isomer, because the PCy_2 resonances are split at temperatures higher than the P_2 resonances, in spite of their more similar frequencies. Out of these three isomers, one of them gives P_2 resonances at −46.5 and −127.7 ppm strongly coupled to each other (J_{PP} = 470 Hz) and is thus assigned to an isomer of type **VII**. The second well-defined isomer gives P_2 resonances at 38.3 and −317.6 ppm with a much reduced P−P coupling of 229 Hz, and it must therefore correspond to an isomer of type **VI** defining an acute P−P−Pb angle. We note, however, that the PCy_2 resonance for this isomer is unusually deshielded (δ_P 213.5 ppm) compared to all other compounds reported in this work. We have previously found in different dicarbonyl complexes of the type $[M_2Cp_2(\mu\text{-}PR_2)_2(CO)_2]$ (M = Mo, W) that the *cis* isomers display ^{31}P NMR shifts much higher (by ca. 45 ppm) than their *trans* isomers.[27,28] Based on this empirical trend, we tentatively propose that the isomer **VI** of compound **7** displays a cisoid (rather than transoid) arrangement of the MCp(CO) fragments. The third isomer of **7** (labeled as **X** in the Experimental Section) gives rise to broad diphosphorus resonances at ca. −100 and −208 ppm and presently we cannot advance a sensible structural proposal for it.

Fluxionality of the Diphosphorus Ligand in Compounds 4 to 8. As discussed in the previous sections, the heterometallic complexes **5** to **8** display in its dominant (or unique) isomer an ER_3 fragment unusually linked to the diphosphorus ligand so as to define an acute P−P−E angle close to 80° (isomer of type **VI**). These molecules undergo a fluxional process in solution that renders equivalent environments for the P atoms of the diphosphorus ligand as well as for the pairs of CO or Cp ligands. From the coalescence temperatures of the corresponding Cp resonances in each case [206 K (**5**), 186 K (**6**), and 180 K (**8**)] we have been able to estimate the corresponding Gibbs free energy barriers,[20] these having fairly low values of 38.6 ± 0.5 (**5**), 35.1 ± 0.5 (**6**), and 35.0 ± 0.5 (**8**) kJ/mol. These barriers are a bit higher than the one determined for the anion **2** (26 kJ/mol), as expected, and not very different from those measured in some organophosphorus molecules having $SnPh_3$ groups. For instance, the stannyl group has been found to shift between P atoms in the 1,2,4-triphosphole $(Ph_3Sn)P_2C_2(^tBu)_2P$, with an activation energy of only 31.5 ± 1 kJ/mol.[33] Moreover, in the 1,3-diphosphole $(Ph_3Sn)P_2C_3(^tBu)_3$, it has been even proposed, based on DFT-calculations, that the stannyl group can exchange positions not only between the P atoms but also with the other C atoms of the diphosphole ring.[32b] We can also quote the niobium complex $[(\eta^2\text{-}Ph_3SnP_3)Nb(ODipp)_3]$, where the stannyl group exchanges its position between the three P atoms.[34]

We have investigated the fluxional rearrangement in our complexes through DFT calculations both on the model tin compound $[Mo_2Cp_2(\mu\text{-}\kappa^2\text{:}\kappa^2\text{-}P_2SnH_3)(\mu\text{-}PCy_2)(CO)_2]$ (**6-H**) and on the simplest diphosphenyl compound $[Mo_2Cp_2(\mu\text{-}\kappa^2\text{:}\kappa^2\text{-}P_2H)(\mu\text{-}PCy_2)(CO)_2]$ (**A**) mentioned earlier. In our preliminary study, we noticed that the DFT-optimized structure of **6-H** was quite similar to that of **6**, with a computed P−P−Sn angle of 89.2°.[10] As for the structure of **A**, we have now found that, surprisingly, it also displays a similar structure of type **VI**, with an acute P−P−H angle of 81.7° and a large P−P separation of 2.183 Å (Table 1 and Supporting Information). In both cases, we were able to find similar transition states, but not the one with C_2 symmetry that it might have been expected, with the X group (X = H, SnH_3) symmetrically bridging the P−P edge: although the diphosphorus ligand in the transition state is found indeed at nearly half way of the swing around the Mo−Mo axis, as proposed for the anion **2** (Scheme 1), the SnH_3 or H atoms have been already transferred to the second P atom, whereas the Cp and CO ligands are at less than half the way from the required rearrangement (Figure 6 and Supporting Information), with M−M−CO angles of 105 and 90° (compare with ca. 115 and 80° in the stationary structures). The computed Gibbs free energies in the gas phase for these transition states are fairly low, 35.8 (**TS-6-H**) and 39.3 kJ/mol (**TS-A**), in excellent agreement with the experimental values for compounds **5**, **6**, and **8** given above.

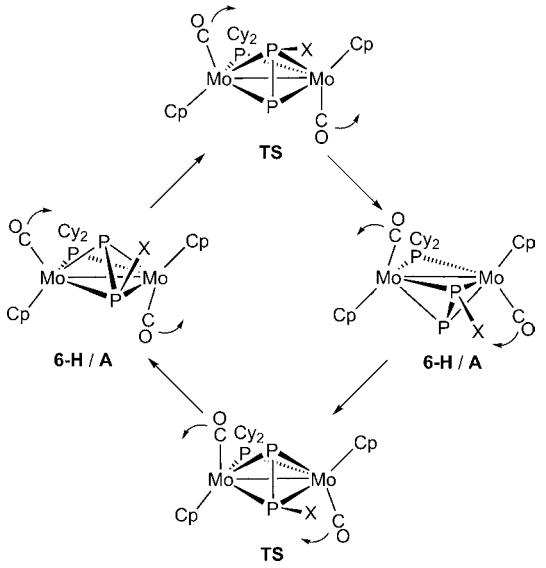

Figure 6. Schematic representation of the DFT-computed fluxionality in compounds $[Mo_2Cp_2(\mu\text{-}\kappa^2\text{:}\kappa^2\text{-}P_2X)(\mu\text{-}PCy_2)(CO)_2]$ (X = H (isomer **A** of compound **4**) or SnH_3 (isomer **VI** of compound **6-H**)).

Once the dynamic behavior of the diphosphenyl complex **A** has been established, we are now in a position to rationalize the observed fluxionality of its agostic isomer **4**, also implying the chemical equivalence of the Cp ligands in the fast exchange limit (Figure 7). For this we only have to find the transition state connecting both isomers. Such a state (**TS-4**) was found to be 81.5 kJ/mol higher than the ground state and represents an intermediate stage with the H atom almost terminally bound to the basal P atom (P−H = 1.413, Mo−H = 3.154, Sn−P = 2.614 Å) but still displaying a large P−P−H angle of 121.4°, while the P−P length remains short (2.119 Å). Actually, such a structure is not very far away from a geometry of type **I**. Therefore we propose that the agostic complex **4** first rearranges into this transient structure that in turn evolves by closing the P−P−H angle and relaxing the P−P length to give the nonagostic isomer **A**, the latter allowing for the H-shift between P atoms as discussed above. Since the kinetic barrier for the isomerization **4** →**A** is the highest one, it defines the overall kinetic barrier for the fluxional process of **4**, which can be compared to the value of 60.5 kJ/mol calculated from the coalescence of the Cp resonances. We note that the transformation **4**/**A** is equivalent to the isomerism actually observed for the tin complex **6** and represents the simplest model for the isomerization between diphosphorus complexes displaying both type **VI** and type **VII** geometries.

Structure and Bonding in Neutral Derivatives of the Anion 2. In our preliminary report on the formation of neutral derivatives of **2** we were able to show, based on DFT calculations on **2**, **3a**, and **6**,[10] that the geometries of the types **I** and **VI** (Chart 1) were the result of different orbital interactions between the incoming electrophile and the anion **2**. In the formation of **3a** (type **I**), the interacting orbital of **2** is the HOMO−2, with substantial lone pair character of the basal P atom (Figure 8), hence a conventional P−P−C angle above 120° follows. This orbital has no participation of the second P atom, therefore explaining that the P−P length retains its π bonding component (see later) and remains as short as found in the anion **2**. At the same time, the removal of nonbonding electron density at the basal atom reinforces the bonding interactions with the dimetal center, in agreement with the selective shortening of the Mo−P(basal) lengths observed upon methylation of **2** (Table 1).

In marked contrast to the above behavior, in the formation of **6** (structure of type **VI**) the interacting orbital of the anion **2** is the HOMO−7, with some participation of the HOMO−1. The former orbital has both σ(Mo−P) and π(P−P) bonding character (hence the short P−P length in **2**). Actually, this orbital can be viewed as resulting from the interaction of one of the π bonding orbitals of a P≡P molecule with a suitable acceptor orbital of the unsaturated anion **1**. As a result, the P−P length must be elongated upon attachment of the ER_3^+ cation, in agreement with the geometrical data for **5** and **6** (Table 1) and with the strong reduction of the P−P coupling observed for all these products. Moreover, this interaction explains that the added electrophiles are positioned at nearly right angles with respect to the P−P bond, because it is in that position where the orbital overlaps with HOMO−7 and HOMO−1 are maximized. We must stress that the σ(P−P) bonding orbital

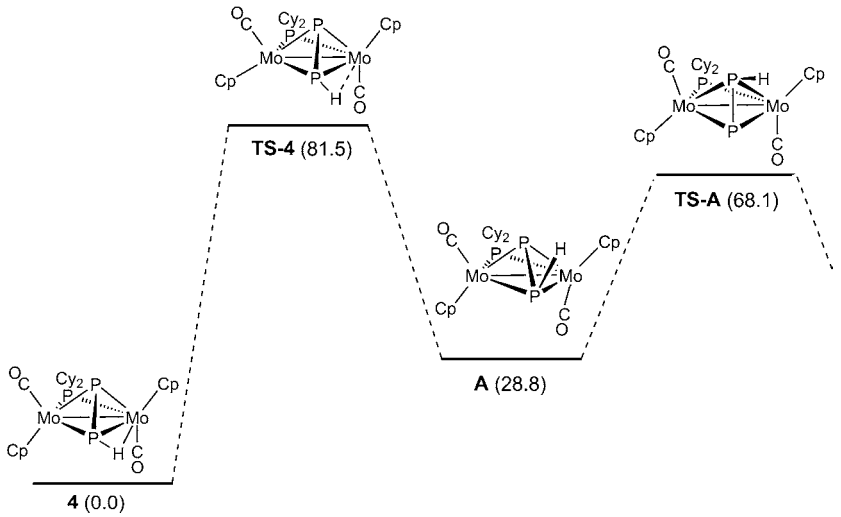

Figure 7. Schematic profile for the fluxional process proposed for the agostic diphosphenyl complex **4**, with DFT-computed Gibbs free energies in kJ/mol given in brackets (only half of the symmetrical process is shown).

dx.doi.org/10.1021/ic301612g | *Inorg. Chem.* 2012, 51, 11061−11075

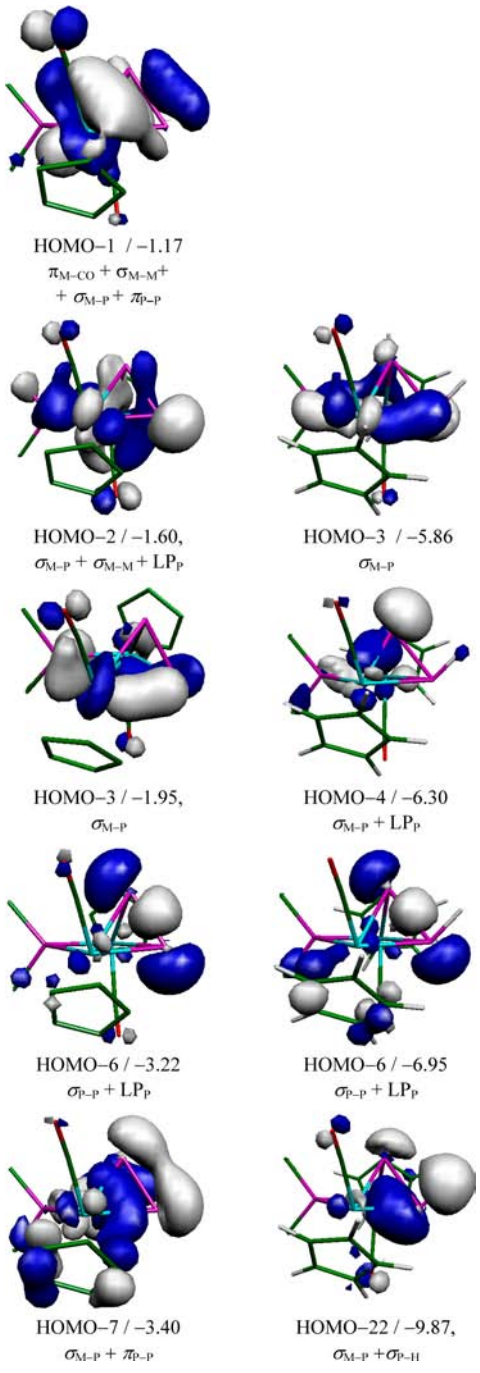

Figure 8. Selected Khon-Sham molecular orbitals of the anion **2** (left, with H omitted) and selected orbitals involving the diphosphenyl ligand in **A** (right), with their energies (in eV) and main bonding character indicated below. The H atoms and Cy groups (except the C^1 atoms) have been omitted for clarity.

(HOMO−6) is not involved at all in the above interaction (actually, the position of attachment of the ER_3 group is close to the nodal plane of that orbital, see Figure 8). Thus we can properly speak of a peculiar π-donor-like ability of the diphosphorus ligand in the anion **2**.

The fact that the structure now computed for the diphoshenyl complex **A** (Table 1) is comparable to that of the stannyl compound **6**, rather than to the structure of the methyldiphosphenyl complex **3a**, would have defied any prediction, considering the greater similarity of the proton with the methyl cation. An inspection of the molecular orbitals of **A** (Figure 8, right) reveals that the situation is indeed comparable to that of the tin compound **6**: the new P−H bond (HOMO−22 in **A**) is mainly derived from the interaction of the 1s orbital of hydrogen with the HOMO−7/HOMO−1 orbitals of **2**, thus destroying the π-component of the P−P bond without involving the σ(P−P) bond (HOMO−6 in **A**). The LP at the basal P atom, represented by the HOMO−2 in **2**, becomes widely distributed among different orbitals upon protonation but still is not involved in bonding with the H atom. Indeed, separate natural bond orbitals (NBOs)[35] could be found representing each of the lone electron pairs at the phosphorus atoms, in addition to the P−P and P−H bonds in **A** (Figure 9).

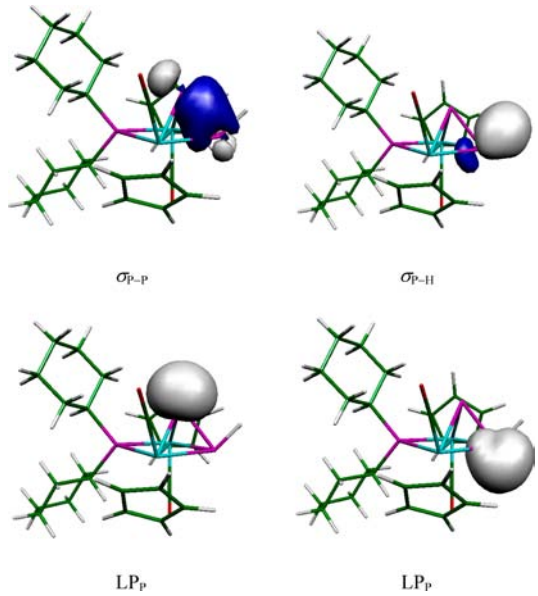

Figure 9. Selected NBO orbitals involving the diphosphenyl ligand in **A**.

The different orbital interactions involved in the formation of derivatives of type **I** or **VI** from **2** also have dramatic consequences on the chemical shielding of the P atoms of the diphosphorus ligand, as noted above (Table 3). Our calculations indicate that the diamagnetic contribution to the shielding at the basal and apical P atoms are comparable in all compounds, but the paramagnetic contribution, associated *inter alia* to the asymmetry of the electron density surrounding each nucleus, can be very different (by several hundreds of ppm) at the basal and apical atoms. This might have been hardly anticipated for the apical P atom, considering that it is not directly involved in any bonding interaction with the incoming electrophile. Moreover we must note that the paramagnetic contribution is modified in opposite ways when comparing type **I** and type **VI** compounds, to yield and ordering in their absolute values of **3a** < **2** < **6** ≪ **A** for the apical position but **3a** > **2** > **6** > **A** for the basal position (Table 3). Presently we cannot give even a qualitative explanation for these trends.

The formation of derivatives of type **VII** (including the agostic diphosphenyl complex **4**) can be rationalized by considering the interaction of the acceptor orbital of the electrophile with a high-energy orbital of the anion **2** having large Mo−P(basal) bonding character. Those conditions are nicely met by the HOMO−3 orbital of **2**, and the resulting

dx.doi.org/10.1021/ic301612g | *Inorg. Chem.* 2012, 51, 11061−11075

tricentric interaction is completely analogous to that involved in the formation of agostic HPR_2 complexes upon protonation of the Mo−P bonds of PR_2-bridged dimolybdenum complexes of the type $[Mo_2Cp_2(\mu\text{-}PR_2)_2(CO)_2]$.[28] As we have seen above, this tricentric interaction leads to the most stable isomer when the electrophile is a proton but gives a less stable isomer (compared to those of type **VI**) for the metal-based electrophiles ER_3, perhaps because of steric effects derived from the close proximity of the bulky ER_3 groups to the metal center.

Since the bicentric orbital interactions behind the formation of structures of type **I** and **VI** are possible for all the electrophiles considered in this work, the question remains as for what reason **3a** displays a type **I** structure and not one of type **VI** or the reverse, e.g. why is it that the nonagostic diphosphenyl complex **A** would adopt a structure of type **VI** and not one of type **I**. To answer this question first we scanned the potential energy surface of **A** in search for a structure of type **I** by using better-quality basis sets for the H atom bound to P but failed to find a minimum with such a geometry. We have mentioned above that a type **I** geometry neither was a minimum for the model stannyl compound **6-H**. Another calculation was performed for **3a** in search for a structure of type **VI**, but again no minimum with this sort of geometry was found. Since no significant steric effects are involved in the case of the unsubstituted diphosphenyl ligand, then we conclude that the orbital interactions tend to intrinsically favor the structure of type **VI** over that of type **I** for the neutral derivatives of **2**, thus explaining its prevalence in the heavy ER_3 derivatives. For the lighter C-based electrophiles, we trust that the structure of type **VI** is disfavored just on steric grounds: because of the small covalent radius of carbon, the H atoms of a hypothetical methyl group placed at acute P−P−CH_3 angles of ca. 85° are computed to get too close to the apical P atom (2.2−2.6 Å, depending on orientation), clearly beyond the van der Waals limits (ca. 3.1 Å). Of course, this effect would be much worse for a benzyl group as found in **3b**. In all, it seems that the particular structure adopted by the neutral derivatives of **2** follows from a delicate balance of steric and electronic effects operating in opposite directions, with the orbital interactions being more favorable in the order **VII** > **VI** > **I** and the steric effects disfavoring these structures in the same order, thus yielding the reverse order of stability (**VII** < **VI** < **I**). It remains to be seen if other heterometallic derivatives of the anionic diphosphorus complex **2** will follow these trends, and further work in that direction is being carried out currently in our laboratory.

CONCLUDING REMARKS

The basal atom of the diphosphorus ligand in the anion **2** has three distinct ways of interacting with a simple electrophile (E^+), to yield derivatives of the types **I**, **VI**, and **VII** represented in Chart 1: The first one (**I**) is dominant for C-based electrophiles, involves the expected electron donation of the lone pair of P to the acceptor orbital of the electrophile, leads to a positioning of the latter at obtuse P−P−E angles above 120°, and does not modify the strong P−P bond of the diphosphorus ligand. The second one (**VI**) is dominant for all other electrophiles investigated in this work (excluding the proton), involves high-energy molecular orbitals of the anion **2** having both σ(Mo−P) and π(P−P) bonding character, without involving the lone electron pair at phosphorus or its σ(P−P) bonding orbital, and thus represents a new and peculiar π-donor-like ability of the diphosphorus ligand. This novel coordination mode of the P_2 ligand has different consequences: (1) the electrophile is positioned at acute P−P−E angles close to 90° so that orbital overlap is maximized; (2) the P−P bond is significantly weakened (hence elongated P−P lengths and largely reduced P−P couplings); (3) a strong shielding of the basal P nucleus and deshielding of the apical P nucleus occur, due to the dramatic alterations in the corresponding paramagnetic contributions to the chemical shielding; and (4) an easy exchange of the added electrophile between the inequivalent P atoms of the diphosphorus ligand follows. The third interaction mode (**VII**) involves a high-energy orbital of the anion having σ(Mo−P) bonding character of the basal P atom, leads to a novel tricentric Mo−E−P interaction with little perturbation of the P−P bond, and is dominant in the absence of steric effects (E = H). The agostic M−H−P interaction leads to ^{1}H chemical shifts and H−P couplings very similar to the values expected for the corresponding hydride isomers, thus precluding a correct structural identification of this sort of interactions only based on NMR spectroscopy.

EXPERIMENTAL SECTION

General Procedures and Starting Materials. All manipulations and reactions were carried out under a nitrogen (99.995%) atmosphere using standard Schlenk techniques. Solvents were purified according to literature procedures and distilled prior to use.[36] Tetrahydrofuan solutions of compound $Li[Mo_2Cp_2(\mu\text{-}PCy_2)(\mu\text{-}CO)_2]$ (**1**) were prepared in situ as described previously,[12b] and all other reagents were obtained from the usual commercial suppliers and used as received, unless otherwise stated. Petroleum ether refers to that fraction distilling in the range 338−343 K. Chromatographic separations were carried out using jacketed columns refrigerated by tap water (ca. 288 K). Commercial aluminum oxide (activity I, 150 mesh) was degassed under vacuum prior to use. The latter was mixed under nitrogen with the appropriate amount of water to reach the activity desired. IR stretching frequencies of CO ligands were measured in solution (using CaF_2 windows) and are referred to as ν(CO). Nuclear magnetic resonance (NMR) spectra were routinely recorded at 300.13 (^{1}H), 121.50 (^{31}P{^{1}H}), or 75.47 MHz (^{13}C{^{1}H}) at 298 K in CD_2Cl_2 solution unless otherwise stated. Chemical shifts (δ) are given in ppm, relative to internal tetramethylsilane (^{1}H, ^{13}C) or external 85% aqueous H_3PO_4 solutions (^{31}P). Coupling constants (J) and line widths at half intensity of broad peaks ($\Delta\nu_{1/2}$) are given in Hertz. The P atoms of the diphosphorus ligands are labeled as P^{bs} and P^{ap}, with P^{bs} being the P atom closer to the "basal" $Mo_2P(Cy_2)$ plane.

Preparation of Tetrahydrofuran Solutions of $Li[Mo_2Cp_2(\mu\text{-}PCy_2)(CO)_2(\mu\text{-}\kappa^2\text{:}\kappa^2\text{-}P_2)]$ (Li-2). A solution of P_4 in toluene (0.9 mL of a ca. 0.18 M solution, 0.162 mmol) was added into a Schlenk tube equipped with a J-Young-type Teflon stopper, and the solvent was then removed under vacuum to leave a white residue of solid P_4. A freshly prepared tetrahydrofuran (THF) solution (10 mL) of compound **1** (containing ca. 0.156 mmol) was then transferred using a canula to the former Schlenk tube, and the mixture was stirred for 30 min at room temperature to give a red-yellowish solution containing a slight excess of P_4 and compound **Li-2** ready for further use. Compound **Li-2** turned out to be highly air sensitive, and all attempts to isolate it as a pure solid led to its progressive decomposition. ^{31}P{^{1}H} NMR [THF/C_6D_6 (10/1), 161.97 MHz, 298 K]: δ 166.7 (s, PCy_2), −166.4 (br, P_2). ^{31}P{^{1}H} NMR [THF/C_6D_6(10/1), 161.97 MHz, 243 K]: δ 166.2 (s, PCy_2), −170.0 (vbr, P_2). ^{31}P{^{1}H} NMR [THF/C_6D_6 (10/1), 161.97 MHz, 183 K]: δ 166.7 (s, PCy_2) ppm, no signal was observed for the P_2 moiety. ^{31}P{^{1}H} NMR [THF/C_6D_6 (10/1), 161.97 MHz, 163K]: δ 165.3 (s, PCy_2), −80.0 (vbr, P^{ap}), −273.0 (vbr, P^{bs}).

Preparation of Tetrahydrofuran Solutions of [PPN]-$[Mo_2Cp_2(\mu\text{-}PCy_2)(CO)_2(\mu\text{-}\kappa^2\text{:}\kappa^2\text{-}P_2)]$ (PPN-2). Solid $[(PPh_3)_2N]Cl$ (0.017 g, 0.040 mmol) was added to a solution containing ca. 0.035

dx.doi.org/10.1021/ic301612g | Inorg. Chem. 2012, 51, 11061−11075

mmol of **Li-2** prepared as described above, and the mixture was stirred for 1 min to give a red solution of **PPN-2** as the major species. All attempts to isolate or purify this extremely air-sensitive compound invariably led to its rapid decomposition.

Preparation of Tetrahydrofuran Solutions of [Li(12-crown-4)$_2$][Mo$_2$Cp$_2$(μ-PCy$_2$)(CO)$_2$(μ-κ^2:κ^2-P$_2$)] ([Li(12-crown-4)$_2$]-2). Neat 12-crown-4 ether (90 μL, 0.556 mmol) was added to a solution containing ca. 0.035 mmol of **Li-2** prepared as described above, and the mixture was stirred for ca. 5 min until complete disappearance of the 1769 cm^{-1} band of **Li-2** was observed, to give a solution containing [**Li(12-crown-4)$_2$**]-**2** as the major organometallic species. All attempts to isolate or purify this extremely air-sensitive compound invariably led to its rapid decomposition.

Preparation of [Mo$_2$Cp$_2$(μ-κ^2:κ^2-P$_2$Me)(μ-PCy$_2$)(CO)$_2$] (3a). Neat MeI (10 μL, 0.16 mmol) was added to a freshly prepared solution of **Li-2** (ca. 0.060 mmol) in tetrahydrofuran (8 mL), and the mixture was stirred for 5 min at room temperature to give a red solution. The solvent was then removed under vacuum, the residue was extracted with dichloromethane-petroleum ether (1:5), and the extracts were chromatographed through alumina (activity IV). A red fraction was eluted using the same mixture of solvents which gave, upon removal of solvents, compound **3a** as an air-sensitive red solid (0.020 g, 51%). Anal. Calcd for $C_{25}H_{35}Mo_2O_2P_3$: C, 46.03; H, 5.41. Found: C, 45.85; H, 5.34. ^{1}H NMR: δ 5.23 (dt, J_{HP} = 1, 0.5, 5H, Cp), 5.19 (dd, J_{HP} = 2, 1, 5H, Cp), 1.99 (ddd, J_{HP} = 11, 4, 0.6, 3H, Me), 2.0−1.1 (m, 22H, Cy). ^{31}P NMR: δ 156.9 (m, br, PCy$_2$), −84.3 (dm, $^1J_{PP}$ = 503, PMe), −293.2 (dd, J_{PP} = 503, 13, P^{ap}). ^{13}C{^{1}H} NMR: δ 239.0 (m, CO), 237.8 (m, CO), 89.3(s, Cp), 86.0 (d, J_{CP} = 2, Cp), 51.7 (dd, J_{CP} = 14, 3, C^1−Cy), 44.7 (d, J_{CP} = 9, C^1−Cy), 36.1 (d, J_{CP} = 4, C^2−Cy), 36.0 (d, J_{CP} = 3, C^2−Cy), 35.0 (d, J_{CP} = 7, C^2−Cy), 34.7 (d, J_{CP} = 5, C^2−Cy), 29.0 (d, J_{CP} = 11, C^3−Cy), 28.7 (d, J_{CP} = 11, C^3−Cy), 28.5 (d, J_{CP} = 9, C^3−Cy), 28.4 (d, J_{CP} = 10, C^3−Cy), 26.8 (d, J_{CP} = 2, C^4−Cy), 26.8 (s, C^4−Cy), −5.6 (dt, J_{CP} = 26, 4, PMe).

Preparation of [Mo$_2$Cp$_2$(μ-κ^2:κ^2-P$_2$CH$_2$Ph)(μ-PCy$_2$)(CO)$_2$] (3b). Neat ClCH$_2$Ph (50 μL, 0.435 mmol) was added to a freshly prepared solution of **Li-2** (ca. 0.070 mmol) in tetrahydrofuran (8 mL), and the mixture was stirred for 3 h at room temperature to yield a red solution. The solvent was then removed under vacuum, the residue was extracted with dichloromethane/petroleum ether (1/4), and the extracts were chromatographed through alumina (activity IV). A red fraction was eluted using the same mixture of solvents which gave, upon removal of solvents, compound **3b** as an air-sensitive red solid (0.025 g, 49%). Anal. Calcd for $C_{31}H_{39}Mo_2O_2P_3$: C, 51.11; H, 5.40. Found: C, 51.33; H, 5.55. ^{1}H NMR: δ 7.30−7.17 (m, 5H, Ph), 5.15 (dd, J_{HP} = 1.7, 0.8, 5H, Cp), 4.95 (d, J_{HP} = 1, 5H, Cp), 3.75 (ABMX, J_{HH} = 13, J_{HP} = 11, 3, 1H, CH$_2$), 3.65 (ABMXZ, J_{HH} = 13, J_{HP} = 5.5, 1, 1, 1H, CH$_2$), 2.0−1.0 (m, 22H, Cy). ^{13}C{^{1}H} NMR (100.63 MHz): δ 238.8 (dt, J_{CP} = 33, 7, CO), 237.7 (m, CO), 140.7 (d, J_{CP} = 10, C^1−Ph), 129.4 (d, J_{CP} = 7, C^2−Ph), 128.8 (d, J_{CP} = 3, C^3−Ph), 126.8 (d, J_{CP} = 4, C^4−Ph), 89.3, 85.8 (2s, Cp), 51.6 (dd, J_{CP} = 13, 3, C^1−Cy), 44.7 (d, J_{CP} = 9, C^1−Cy), 36.1 (d, J_{CP} = 3, 2C^2−Cy), 35.0 (d, J_{CP} = 7, C^2−Cy), 34.5 (d, J_{CP} = 5, C^2 -Cy), 29.0 (d, J_{CP} = 11, C^3−Cy), 28.7 (d, J_{CP} = 11, C^3−Cy), 28.5 (d, J_{CP} = 9, 2C^3−Cy), 26.8, 26.7 (2s, C^4−Cy), 17.6 (dt, J_{CP} = 34, 4, PCH$_2$).

Preparation of [Mo$_2$Cp$_2$(μ-PCy$_2$)(CO)$_2$(μ-κ^2:κ^1,η^2-HP$_2$)] (4). Neat BrSiMe$_3$ (30 μL, 0.227 mmol) was added to a freshly prepared solution of **Li-2** (ca. 0.156 mmol) in tetrahydrofuran (10 mL), and the mixture was stirred for 10 min at room temperature to yield a yellow-brown solution. The solvent was then removed under vacuum, the residue was extracted with petroleum ether, and the extracts were filtered through diatomaceous earth. Removal of solvents from the filtrate gave a yellow-green solid (0.050 g, ca. 50%) containing **4** as the major species (ca. 95%), along with very small amounts of other uncharacterized species. All attempts to further purify this product led to its progressive decomposition. ν(CO) (petroleum ether): 1896 (w), 1877 (vs) cm^{-1}. ^{1}H NMR (toluene-d_8, 400.13 MHz, 308 K): δ 4.74 (s, $\Delta\nu_{1/2}$ = 7, 10H, Cp), 2.5−1.0 (m, 22H, Cy), −10.04 (d, J_{PH} = 8, 1H, Mo−H−P). ^{1}H NMR (tol-d_8, 400.13 MHz, 298 K): δ 4.72 (s, br, $\Delta\nu_{1/2}$ = 16, 10H, Cp), 2.5−1.0 (m, 22H, Cy), −10.05 (d, J_{PH} = 8, 1H, Mo−H−P). ^{1}H NMR (tol-d_8, 400.13 MHz, 258 K): δ 4.71, 4.59 (2s, 2 × 5H, Cp), 2.5−1.0 (m, 22H, Cy), −10.07 (ddd, J_{PH} = 8.8, 4.4, 3.4, 1H, Mo−H−P). ^{31}P{^{1}H} NMR (toluene-d_8, 161.96 MHz, 258 K): δ 141.5 (t, J_{PP} = 6, PCy$_2$), −129.1 (d, J_{PP} = 461, P^{ap}), −315.4 (d, J_{PP} = 461, P^{bs}). ^{13}C{^{1}H} NMR (toluene-d_8, 100.63 MHz, 258 K): δ 238.1 (m, CO), 233.0 (dd, J_{CP} = 26, 9, CO), 89.0, 84.9 (2s, Cp), 51.3 (d, J_{CP} = 13, C^1−Cy), 45.1 (d, J_{CP} = 11, C^1−Cy), 36.1 (d, J_{CP} = 2, C^2−Cy), 35.7 (d, J_{CP} = 8, C^2−Cy), 34.9 (d, J_{CP} = 4, C^2−Cy), 34.8 (d, J_{CP} = 4, C^2−Cy), 28.8 (d, J_{CP} = 11, C^3−Cy), 28.7 (d, J_{CP} = 9, C^3−Cy), 28.4 (d, J_{CP} = 10, C^3−Cy), 28.2 (d, J_{CP} = 9, C^3−Cy), 26.8, 26.6 (2s, C^4−Cy).

Preparation of [Mo$_2$Cp$_2$(μ-κ^2:κ^2-P$_2$GePh$_3$)(μ-PCy$_2$)(CO)$_2$] (5). Solid ClGePh$_3$ (0.075 g, 0.220 mmol) was added to a freshly prepared solution of **Li-2** (ca. 0.156 mmol) in tetrahydrofuran (10 mL), and the mixture was stirred for 5 min to give an orange solution. The solvent was then removed under vacuum, the residue was extracted with tetrahydrofuran/petroleum ether (1/5, 3 × 6 mL), and the extracts were filtered. Removal of solvents from the filtrate gave compound **5** as an orange residue. This was further purified by the slow diffusion at 253 K of a layer of petroleum ether (6 mL) into a concentrated toluene solution (3 mL) of the crude product, this yielding crystals of **5** suitable for the X-ray analysis (0.053 g, 36%). Anal. Calcd for $C_{42}H_{47}GeMo_2O_2P_3$: C, 53.59; H, 5.03. Found: C, 53.38; H, 4.97. ^{1}H NMR (300.09 MHz): δ 7.61−7.54 (m, 6H, Ph), 7.42−7.36 (m, 9H, Ph), 5.00 (q, J_{HP} = 0.9, 10H, Cp), 2.0−1.1 (m, 22H, Cy). ^{1}H NMR (400.13 MHz, 298 K): δ 7.60−7.56 (m, 6H, Ph), 7.41−7.35 (m, 9H, Ph), 5.00 (s, 10H, Cp), 2.05−1.10 (m, 22H, Cy). ^{1}H NMR (400.13 MHz, 218 K): δ 7.61−7.56 (m, 6H, Ph), 7.46−7.38 (m, 9H, Ph), 5.00 (s, br, $\Delta\nu_{1/2}$ ≈ 53, Cp, 10H), 1.96−1.04 (m, 22H, Cy). ^{1}H NMR (400.13 MHz, 178 K): δ 7.62−7.55 (m, 6H, Ph), 7.49−7.39 (m, 9H, Ph), 5.36, 4.62 (2s, 2 × 5H, Cp), 1.96−1.04 (m, 22H, Cy). ^{31}P{^{1}H} NMR (161.98 MHz, 298 K): δ 143.9 (s, PCy$_2$), −159 (vbr, $\Delta\nu_{1/2}$ ≈ 2500, P$_2$). ^{31}P{^{1}H} NMR (161.98 MHz, 238 K): δ 141.4 (s, PCy$_2$), −7 (vbr, P^{ap}), −293 (vbr, PGe). ^{31}P{^{1}H} NMR (161.98 MHz, 218 K): δ 140.5 (s, PCy$_2$), 4 (br, $\Delta\nu_{1/2}$ ≈ 750, P^{ap}), −301 (br, $\Delta\nu_{1/2}$≈ 740, PGe). ^{31}P{^{1}H} NMR (161.98 MHz, 178 K): δ 138.6 (s, PCy$_2$), 27.5 (d, br, J_{PP} ≈ 280, P^{ap}, isomer **VI**), 7 (br, P^{ap}, rotamer of **VI**), −299 (br, PGe, rotamer of **VI**), −315.5 (br, J_{PP} ≈ 280, PGe, isomer **VI**): ratio **VI**/rotamer ca. 13. ^{13}C{^{1}H} NMR (100.63 MHz, 298 K, isomer **VI**): δ 237.5 (dd. J_{CP} = 19, 9, CO), 139.2 (t, J_{CP} = 7, C^1−Ph), 135.1 (s, C^2−Ph), 129.6 (s, C^4−Ph), 128.6 (s, C^3−Ph), 87.9 (s, Cp), 47.9 (d, J_{CP} = 12, C^1−Cy), 35.3 (d, J_{CP} = 3, C^2−Cy), 35.0 (s, C^2−Cy), 28.7 (d, J_{CP} = 12, C^3−Cy), 28.4 (d, J_{CP} = 9, C^3−Cy), 26.7 (s, C^4). ^{13}C{^{1}H} NMR (400.13 MHz, 178 K): δ 238.3 (d, br, J_{CP} = 37, CO), 237.3 (br, CO), 139.3 (dd, J_{CP} = 8, 3, C^1−Ph), 134.8 (s, C^2−Ph), 129.6 (s, C^4−Ph), 128.5 (s, C^3−Ph), 90.4, 85.3 (2s, Cp), 50.6 (br, C^1−Cy), 36.6, 34.0, 33.7, 32.0 (4s, br, C^2−Cy), 28.5−27.5 (4s, br, C^3−Cy), 26.5, 26.4 (2s, C^4−Cy).

Preparation of [Mo$_2$Cp$_2$(μ-κ^2:κ^2-P$_2$SnPh$_3$)(μ-PCy$_2$)(CO)$_2$] (6). Solid ClSnPh$_3$ (0.060 g, 0.156 mmol) was added to a freshly prepared solution of **Li-2** (ca. 0.06 mmol) in tetrahydrofuran (8 mL), and the mixture was stirred for 5 min at room temperature to yield a red orange solution. The solvent was then removed under vacuum, the residue was extracted with dichloromethane/petroleum ether (1/9), and the extracts were chromatographed through alumina (activity IV). An orange fraction was eluted using the same mixture of solvents which gave, upon removal of solvents, compound **6** as an orange microcrystalline solid (0.035 g, 59%). Anal. Calcd for $C_{42}H_{47}Mo_2O_2P_3Sn$: C, 51.09; H, 4.80. Found: C, 50.88; H, 4.92. ^{1}H NMR (400.13 MHz, 298 K): δ 7.66 (m, $J_{H\text{-}119/117Sn}$ ≈ 52, 6H, *o*-Ph), 7.45−7.30 (m, 9H, Ph), 4.99 (s, 10H, Cp), 2.0−1.1 (m, 22H, Cy). ^{1}H NMR (400.13 MHz, 170 K, isomer **VI**): δ 7.71 (m, $J_{H\text{-}119/117Sn}$ ≈ 52, 6H, *o*-Ph), 7.44 (m, 9H, Ph), 5.32 (br, $\Delta\nu_{1/2}$ = 27, 5H, Cp), 4.66 (br, $\Delta\nu_{1/2}$ = 26, 5H, Cp), 2.2−0.8 (m, 22H, Cy). ^{1}H NMR (400.13 MHz, 170 K, isomer **VII**): δ 5.09, 4.43 (2s, 2 × 5H, Cp), the resonances of the Ph and Cy groups were masked by those of the major isomer **VI** (ratio **VI**/**VII** ca. 9 at 170 K). ^{13}C{^{1}H} NMR (100.63 MHz, 298 K): δ 237.4 (dd, J_{CP} = 16, 9, CO), 142.3 (t, J_{CP} = 8, $J_{C\text{-}119Sn}$ ≈ 470, $J_{C\text{-}117Sn}$ ≈ 450, C^1−Ph), 137.1 (s, $J_{C\text{-}119/117Sn}$ ≈ 40, C^2−Ph), 129.4 (s, $J_{C\text{-}119/117Sn}$ ≈ 13, C^4−Ph), 128.8 (s, $J_{C\text{-}119/117Sn}$ ≈ 52, C^3−Ph), 88.0 (s, Cp), 47.6 (d, J_{CP} = 12, C^1−Cy), 35.3 (d, J_{CP} = 4, C^2−Cy), 34.7 (s, C^2−Cy), 28.7 (d, J_{CP} = 12, C^3−Cy), 28.4 (d, J_{CP} = 10, C^3−Cy), 26.7 (s, C^4). ^{13}C{^{1}H}

dx.doi.org/10.1021/ic301612g | *Inorg. Chem.* 2012, 51, 11061−11075

NMR (100.63 MHz, 178 K, isomer **VI**): δ 239.0 (br, CO), 237.0 (br, CO), 141.8 (t, J_{CP} = 8, $J_{C\text{-}119/117Sn} \approx$ 460, C^1–Ph), 136.9 (s, $J_{C\text{-}119/117S\ n} \approx$ 41, C^2–Ph), 129.5 (s, C^4–Ph), 128.8 (s, $J_{C\text{-}119/117Sn} \approx$ 50, C^3–Ph), 90.4, 85.5 (2s, br, Cp), 51.0 (s, br, C^1–Cy), 37.0, 34.0, 31.5 (3s, br, C^2–Cy), 28.3, 27.9 (2s, br, C^3–Cy), 26.5 (s, C^4). $^{13}C\{^1H\}$ NMR (100.63 MHz, 178 K, isomer **VII**, Cp region): δ 89.0, 87.0 (2s, Cp).

Preparation of $[Mo_2Cp_2(\mu\text{-}\kappa^2\text{:}\kappa^2\text{-}P_2PbPh_3)(\mu\text{-}PCy_2)(CO)_2]$ (7). Solid $ClPbPh_3$ (0.076 g, 0.160 mmol) was added to a freshly prepared solution of **Li-2** (ca. 0.156 mmol) in tetrahydrofuran (10 mL), and the mixture was stirred for 5 min at room temperature to yield an orange-brown solution. The solvent was then removed under vacuum, the residue was extracted with tetrahydrofuran/petroleum ether (1/10, 3 × 11 mL), and the extracts were filtered through diatomaceous earth. The solvents were then removed under vacuum to give a red-brown residue. The latter was extracted with dichloromethane/petroleum ether (1/7), and the extracts were chromatographed through alumina (activity IV). A red fraction was eluted using the same mixture of solvents which gave, upon removal of solvents, compound **7** as an air-sensitive red solid (0.080 g, 51%). Anal. Calcd for $C_{42}H_{47}Mo_2O_2P_3Pb$: C, 46.89; H, 4.40. Found: C, 47.11; H, 4.50. ^1H NMR (400.13 MHz, 298 K): δ 7.68 (m, J_{H-Pb} = 75, 6H *o*-Ph,), 7.41 (m, 6H, *m*-Ph), 7.31 (m, 3H, *p*-Ph), 5.00 (s, Cp, 10H), 2.0–1.1 (m, Cy, 22H). ^1H NMR (400.13 MHz, 218 K, mixture of isomers **VI**, **VII** and **X**): δ 7.73 (m, J_{H-Pb} = 80, *o*-Ph), 7.64 (m, J_{H-Pb} = 54, *o*-Ph), 7.52–7.32 (m, *m*,*p*-Ph), 5.05 (s, Cp, 10H, isomer **VII**), 5.01 (s, br, $\Delta\nu_{1/2} \approx$ 7, Cp, 10H, isomer **VI**), 4.89 (s, br, $\Delta\nu_{1/2} \approx$ 8, Cp, 10H, isomer **X**), 2.4–1.1 (m, Cy). Ratio of isomers **VI**:**VII**:**X** ≈ 1.6:1.2:.0. $^{31}P\{^1H\}$ NMR: δ 142.0 (br, PCy_2), −107.7 (br, P_2). $^{31}P\{^1H\}$ NMR (161.98 MHz, 298 K): δ 142.4 (br, $\Delta\nu_{1/2} \approx$ 600, PCy_2), −107.1 (br, $\Delta\nu_{1/2} \approx$ 700, P_2). $^{31}P\{^1H\}$ NMR (161.98 MHz, 178 K): δ 213.5 (s, PCy_2, isomer **VI**), 142.0 (vbr, PCy_2, isomer **X**), 139.5 (s, PCy_2, isomer **VII**), 57.7 (d, br, $J_{PP} \approx$ 200, P^{ap}, isomer **VI**), −46.5 (d, $J_{PP} \approx$ 470, P^{ap}, isomer **VII**), −100 (vbr, P_2, isomer **X**), −127.7 (d, $J_{PP} \approx$ 470, P^{bs}, isomer **VII**), −208 (vbr, isomer **X**), −279 (vbr, P^{bs}, isomer **VI**). $^{13}C\{^1H\}$ NMR (400.13 MHz, 298 K): δ 237.2 (m, br, CO), 155.3 (s, C^1–Ph), 137.5 (s, $J_{CPb} \approx$ 66, C^2–Ph), 129.6 (s, $J_{C-Pb} \approx$ 68, C^3–Ph), 128.7 (s, $J_{C-Pb} \approx$ 18, C^4–Ph), 88.2 (s, Cp), 47.8 (d, J_{CP} = 10, C^1–Cy), 34.9, 34.8 (2s, C^2–Cy), 28.7 (d, J_{CP}= 13, C^3–Cy), 28.3 (d, J_{CP} = 9, C^3–Cy), 26.8 (s, C^4–Cy).

Preparation of $[Mo_2Cp_2(\mu\text{-}\kappa^2\text{:}\kappa^2\text{-}P_2PbMe_3)(\mu\text{-}PCy_2)(CO)_2]$ (8). Solid $ClPbMe_3$ (0.029 g, 0.101 mmol) was added to a freshly prepared solution of **Li-2** (ca. 0.086 mmol) in tetrahydrofuran (10 mL), and the mixture was stirred for 5 min at room temperature to yield an orange-brown solution. The solvent was then removed under vacuum, the residue was extracted with tetrahydrofuran/petroleum ether (1/10, 3 × 11 mL), and the extracts were filtered. Removal of the solvents from the filtrate yielded an orange solid (0.042 g, ca. 55%) containing compound **8** as the major species (>90%), along with other uncharacterized side-products. All attempts to further purify this compound led to its progressive decomposition. ^1H NMR (toluene-d_8, 400.13 MHz, 298 K): δ 4.99 (s, 10H, Cp), 2.1–1.1 (m, 22H, Cy), 1.20 (t, J_{HP} = 1.3, 9H, Me). ^1H NMR (toluene-d_8, 400.13 MHz, 178 K): δ 4.97, 4.86 (2s, br, 2 × 5H, Cp), 2.3–0.8 (m, 22H, Cy), 1.23 (s, 9H, Me).

X-ray Structure Determination for Compound 5. The X-ray intensity data were collected on an Oxford Diffraction Xcalibur Nova single crystal diffractometer, using CuK_α radiation at 150 K. Images were collected at a 63 mm fixed crystal-detector distance, using the oscillation method, with 1° oscillation and variable exposure time per image (3–12 s). Data collection strategy was calculated with the program CrysAlis Pro CCD.[37] Data reduction and cell refinement were performed with the program CrysAlis Pro RED.[37] An empirical absorption correction was applied using the SCALE3 ABSPACK algorithm as implemented in the program CrysAlis Pro RED. Using the program suite WinGX,[38] the structure was solved using direct methods and refined with full-matrix least-squares on F^2 using SHELXL97.[39] All the positional parameters and the anisotropic temperature factors of all the non-H atoms were refined anisotropically, and all hydrogen atoms were geometrically placed and refined using a riding model. Crystallographic data and structure refinement details for **5** are collected in Table 5.

Table 5. Crystal Data for Compound 5

	5
mol formula	$C_{42}H_{47}GeMo_2O_2P_3$
mol wt	941.18
cryst syst	monoclinic
space group	$P\ 2_1/n$
radiation (λ, Å)	1.54814
a, Å	11.5130(1)
b, Å	27.9599(3)
c, Å	12.1493(1)
α, deg	90
β, deg	90.0304(8)
γ, deg	90
V, Å^3	3910.89(7)
Z	4
calcd density, g cm^{-3}	1.598
absorp coeff, mm^{-1}	7.512
temperature, K	150(2)
θ range (deg)	3.16 to 74.34
index ranges (*h*, *k*, *l*)	−13, 14; −25, 34; −14, 15
no. of reflns collected	22671
no. of indep reflns (R_{int})	7628 (0.0302)
reflns with $I > 2\sigma(I)$	6676
R indexes [data with $I > 2\sigma(I)$][a]	R_1 = 0.0262
	wR_2 = 0.0652[b]
R indexes (all data)[a]	R_1 = 0.0322
	wR_2 = 0.0687[b]
GOF	1.026
no. of restraints/params	0/451
$\Delta\rho$(max., min.), eÅ^{-3}	0.599, −0.674

[a] $R = \Sigma||F_o| - |F_c||/\Sigma|F_o|$. $wR = [\Sigma w(|F_o|^2 - |F_c|^2)^2/\Sigma w|F_o|^2]^{1/2}$. $w = 1/[\sigma^2(F_o^2) + (aP)^2 + bP]$ where $P = (F_o^2 + 2F_c^2)/3$. [b] a = 0.0362, b = 1.3110.

DFT Analysis. All computations described in this work were carried out with the GAUSSIAN03 package,[40] in which the hybrid method B3LYP was applied with the Becke three parameters exchange functional[41]and the Lee–Yang–Parr correlation functional.[42] Effective core potentials (ECP) and their associated double-ζ LANL2DZ basis set were used for the Mo and Sn centers.[43] The light elements (O, C, P, and H) were described with 6-31G* basis.[44] Geometry optimizations were performed under no symmetry restrictions, using initial coordinates derived from X-ray data of the compounds; for the complexes where this information was not available the initial coordinates were obtained by modification of the coordinates of similar complexes. Frequency analyses were performed to ensure that all the stationary points were either a minima (no negative frequencies) or transition states (one negative frequency). NMR shielding contributions and coupling constants were calculated using the gauge-including atomic orbitals (GIAO) method,[45] in combination with the LANL2DZ basis set for the Mo and Sn atoms and the IGLO-III basis set of Kutzelnigg and co-workers for the remaining atoms.[46] Molecular orbitals and vibrational modes were visualized using the Molekel program.[47]

■ ASSOCIATED CONTENT

Ⓢ Supporting Information

A CIF file giving the crystallographic data for the structural analysis of compound **5**. A PDF file containing data (figures, tables of atomic coordinates, selected bond distances and angles, selected molecular orbitals) for the DFT-optimized

structures of compound **4** (isomers **A** to **F**), **6-H** (isomer of type **VII**), and transition states of **4**, **A**, and **6-H** (isomer of type **VI**), and the full ref 40. This material is available free of charge via the Internet at http://pubs.acs.org.

AUTHOR INFORMATION

Corresponding Author

*E-mail: ara_12_79@hotmail.com (A.R.), mara@uniovi.es (M.A.R.).

Notes

The authors declare no competing financial interest.

ACKNOWLEDGMENTS

We thank the DGI of Spain (Project CTQ2009-09444) and the COST action CM0802 "PhoSciNet" for supporting this work.

REFERENCES

(1) (a) Giffin, N. A.; Masuda, J. D. *Coord. Chem. Rev.* **2011**, *255*, 1342. (b) Scheer, M.; Balázs, G.; Seitz, A. *Chem. Rev.* **2010**, *110*, 4236. (c) Quin, L. D. *A Guide to Organophosphorus Chemistry*; Wiley: New York, 2000.

(2) (a) Caporali, M.; Gonsalvi, L.; Rossin, A.; Peruzzini, M. *Chem. Rev.* **2010**, *110*, 4178. (b) Cossairt, B. M.; Piro, N. A.; Cummins, C. C. *Chem. Rev.* **2010**, *110*, 4164. (c) Peruzzini, M.; Gonsalvi, L.; Romerosa, A. *Chem. Soc. Rev.* **2005**, *34*, 1038. (d) Peruzzini, M.; Abdreimova, R. R.; Budnikova, Y.; Romerosa, A.; Scherer, O. J.; Sitzmann, H. *J. Organomet. Chem.* **2004**, *689*, 4319. (e) Peruzzini, M.; de los Rios, I.; Romerosa, A.; Vizza, F. *Eur. J. Inorg. Chem.* **2001**, 593.

(3) Dielmann, F.; Sierka, M.; Virovets, A. V.; Scheer, M. *Angew. Chem., Int. Ed.* **2010**, *49*, 6860.

(4) Scherer, O. J.; Sitzmann, H.; Wolmershäuser, G. *J. Organomet. Chem.* **1984**, *268*, C9.

(5) Vizi-Orosz, A.; Pályi, G.; Markó, L. *J. Organomet. Chem.* **1973**, *60*, C25.

(6) (a) Scherer, O. J.; Sitzmann, H.; Wolmerhauser, G. *J. Organomet. Chem.* **1986**, *309*, 77. (b) Scheer, M.; Schuster, K.; Krug, A.; Hartung, H. *Chem. Ber.* **1996**, *129*, 973. (c) Davies, J. E.; Mays, M. J.; Raithby, P. R.; Shields, G. P.; Tompkin, P. K.; Woods, A. D. *J. Chem. Soc., Dalton Trans.* **2000**, 1925.

(7) (a) Bai, J.; Leiner, E.; Scheer, M. *Angew. Chem., Int. Ed.* **2002**, *41*, 783. (b) Scheer, M.; Gregoriades, L. J.; Zabel, M.; Bai, J.; Krossing, I.; Brunklaus, G.; Eckert, H. *Chem.—Eur. J.* **2008**, *14*, 282.

(8) (a) Abboud, J. L. M.; Herreros, M.; Notario, R.; Esseffar, M.; Mo, O.; Yañez, M. *J. Am. Chem. Soc.* **1996**, *118*, 1126. (b) Abboud, J. L. M.; Alkorta, I.; Dávalos, J. Z.; Gal, J. F.; Herreros, M.; Maria, P. C.; Notario, R.; Mo, O.; Molina, M. T.; Yañez, M. *J. Am. Chem. Soc.* **2000**, *122*, 4451.

(9) Welsch, S.; Lescop, C.; Balazs, G.; Réau, R.; Scheer, M. *Chem.—Eur. J.* **2011**, *17*, 9130.

(10) Alvarez, M. A.; García, M. E.; García-Vivó, D.; Ramos, A.; Ruiz, M. A. *Inorg. Chem.* **2011**, *50*, 2064.

(11) The neutral diphosphorus complex $[Mo_2Cp_2(CO)_3(\mu\text{-}\kappa^2\text{:}\kappa^2\text{-}P_2)(PHPh_2)]$ has been reported to react with DBU and then with several cumulenes and Michael-type acceptors followed by protonation to give mainly products of the type $[Mo_2Cp_2(CO)_3(\mu\text{-}\kappa^2\text{:}\kappa^2\text{-}P_2)(PRPh_2)]$. This presumably involves also the formation of an anionic species but with the negative charge essentially located at the terminal PR_2 ligand. See: (a) Davies, J. E.; Mays, M. J.; Raithby, P. R.; Shields, G. P.; Tompkin, P. K. *Chem. Commun.* **1996**, 2051. (b) Davies, J. E.; Feeder, N.; Mays, M. J.; Tompkin, P. K.; Woods, A. D. *Organometallics* **2000**, *19*, 984.

(12) (a) García, M. E.; Melón, S.; Ramos, A.; Riera, V.; Ruiz, M. A.; Belletti, D.; Graiff, C.; Tiripicchio, A. *Organometallics* **2003**, *22*, 1983. (b) García, M. E.; Melón, S.; Ramos, A.; Ruiz, M. A. *Dalton Trans.* **2009**, 8171.

(13) (a) Koch, W.; Holthausen, M. C. *A Chemist's Guide to Density Functional Theory*, 2nd ed.; Wiley-VCH: Weinheim, 2002. (b) Ziegler, T. *Chem. Rev.* **1991**, *91*, 651. (c) Foresman, J. B.; Frisch, Æ. *Exploring Chemistry with Electronic Structure Methods*, 2nd ed.; Gaussian, Inc.: Pittsburgh, 1996.

(14) Alvarez, M. A.; García, M. E.; Ramos, A.; Ruiz, M. A. *Organometallics* **2007**, *26*, 1461.

(15) Alvarez, M. A.; García, M. E.; Ramos, A.; Ruiz, M. A.; Lanfranchi, M.; Tiripicchio, A. *Organometallics* **2007**, *26*, 5454.

(16) Alvarez, M. A.; García, M. E.; Menéndez, S.; Ruiz, M. A. *Organometallics* **2011**, *30*, 3694.

(17) (a) Darensbourg, M. Y. *Prog. Inorg. Chem.* **1985**, *33*, 221. (b) Darensbourg, M. Y.; Ash, C. E. *Adv. Organomet. Chem.* **1987**, *27*, 1.

(18) Yu, L.; Srinivas, G. N.; Schwartz, M. *J. Mol. Struct. (Theochem)* **2003**, *625*, 215.

(19) Munguia, T.; Bakir, Z. A.; Cervantes-Lee, F.; Metta-Magana, A.; Pannell, K. H. *Organometallics* **2009**, *28*, 5777.

(20) According to the modified Eyring equation $\Delta G^{\#}_{Tc} = 19.14T_c[9.97 + \log(T_c/\Delta\nu)]$ (J/mol). See: Günter, H. *NMR Spectroscopy*; John Wiley: Chichester, U.K., 1980; p 243.

(21) The most common coordination modes for diphosphenyl ligands are κ^1 or $\mu\text{-}\kappa^1\text{:}\kappa^1$; see for instance: Weber, L. *Chem. Rev.* **1992**, *92*, 1839.

(22) (a) Di Vaira, M.; Stoppioni, P.; Midollini, S.; Laschi, F.; Zanello, P. *Polyhedron* **1991**, *10*, 2123. (b) Bencini, A.; Di Vaira, M.; Stoppioni, P.; Uytterhoeven, M. G. *Theor. Chim. Acta* **1995**, *91*, 187.

(23) Cramer, C. J. *Essentials of Computational Chemistry*, 2nd ed.; Wiley: Chichester, U.K., 2004.

(24) Vogler, A.; Hlavatsch, J. *Angew. Chem., Int. Ed. Engl.* **1983**, *22*, 154.

(25) Braterman, P. S. *Metal Carbonyl Spectra*; Academic Press: London, U.K., 1975.

(26) García, M. E.; Riera, V.; Ruiz, M. A.; Rueda, M. T.; Sáez, D. *Organometallics* **2002**, *21*, 5515.

(27) The presence of lone electron pairs on one or both of the coupled nuclei is associated with negative one-bond coupling constants except in coupling to hydrogen atoms. See, for instance: Jameson, C. J. In *Phosphorus-31 NMR Spectroscopy in Stereochemical Analysis*; Verkade, J. G., Quin, L. D., Eds.; VCH: Deerfield Beach, FL, 1987; Chapter 6.

(28) (a) Alvarez, M. A.; García, M. E.; Martinez, M. E.; Ramos, A.; Ruiz, M. A.; Sáez, D.; Vaissermann, J. *Inorg. Chem.* **2006**, *45*, 6965. (b) Alvarez, M. A.; García, M. E.; García-Vivó, D.; Martinez, M. E.; Ruiz, M. A. *Inorg. Chem.* **2009**, *48*, 9767.

(29) Verkade, J. G.; Mosbo, J. A. In *Phosphorus-31 NMR Spectroscopy in Stereochemical Analysis*; Verkade, J. G., Quin, L. D., Eds.; VCH: Deerfield Beach, FL, 1987; Chapter 13.

(30) (a) Schumann, H.; Rodewald, G.; Lefferts, J. L.; Zuckerman, J. *J. Organomet. Chem.* **1980**, *190*, 53. (b) McFarlane, W.; Rycroft, D. S. *J. Chem. Soc., Dalton Trans.* **1974**, 1977.

(31) Alvarez, M. A.; García, M. E.; Ramos, A.; Ruiz, M. A. *Organometallics* **2006**, *25*, 5374.

(32) (a) Grundy, J.; Donnadieu, B.; Mathey, F. *J. Am. Chem. Soc.* **2006**, *128*, 7716. (b) Geoffrey, F.; Cloke, N.; Hitchcock, P. B.; Nixon, J. F.; Wilson, D. J.; Nyulaszi, L.; Karpati, T. *J. Organomet. Chem.* **2005**, *690*, 3983. (c) Schmitz, M.; Goller, R.; Bergstrasser, U.; Leininger, S.; Regitz., M. *Eur. J. Inorg. Chem.* **1998**, 227.

(33) Elvers, A.; Heinemann, F. W.; Wrackmeyer, B.; Zenneck, U. *Chem.—Eur. J.* **1999**, *5*, 3143.

(34) Cossairt, B. M.; Cummins, C. C. *Angew. Chem., Int. Ed.* **2010**, *49*, 1595.

(35) Weinhold, F.; Landis, C. R. *Valence and Bonding*; Cambridge University Press: Cambridge, U.K., 2005.

(36) Armarego, W. L. F.; Chai, C. *Purification of Laboratory Chemicals*, 5th ed.; Butterworth-Heinemann: Oxford, U.K., 2003.

(37) *CrysAlis Pro*; Oxford Diffraction Ltd.: Oxford, U.K., 2006.

(38) Farrugia, L. J. *J. Appl. Crystallogr.* **1999**, *32*, 837.

(39) Sheldrick, G. M. *Acta Crystallogr., Sect. A: Found. Crystallogr.* **2008**, *64*, 112.

(40) Frisch, M. J. et al. *Gaussian 03*, Revision B.02; Gaussian, Inc.: Wallingford, CT, 2004.

(41) Becke, A. D. *J. Chem. Phys.* **1993**, *98*, 5648.
(42) Lee, C.; Yang, W.; Parr, R. G. *Phys. Rev. B* **1988**, *37*, 785.
(43) Hay, P. J.; Wadt, W. R. *J. Chem. Phys.* **1985**, *82*, 299.
(44) (a) Hariharan, P. C.; Pople, J. A. *Theor. Chim. Acta* **1973**, *28*, 213. (b) Petersson, G. A.; Al-Laham, M. A. *J. Chem. Phys.* **1991**, *94*, 6081. (c) Petersson, G. A.; Bennett, A.; Tensfeldt, T. G.; Al-Laham, M. A.; Shirley, W. A.; Mantzaris, J. *J. Chem. Phys.* **1988**, *89*, 2193.
(45) Wolinski, K.; Hinton, J. F.; Pulay, P. *J. Am. Chem. Soc.* **1990**, *112*, 8251.
(46) Kutzelnigg, W.; Fleischer, U.; Schindler, M. *NMR: Basic Princ. Prog.* **1990**, *23*, 165.
(47) Portmann, S.; Lüthi, H. P. *CHIMIA* **2000**, *54*, 766.